



A new era in brain drug delivery: Integrating multivalency and computational optimisation for blood–brain barrier permeation[☆]

Giulia Porro^{a,b,1}, Marco Basile^{a,b,1}, Zhengdong Xie^{a,c,d}, Gian Marco Tuveri^{a,e},
Giuseppe Battaglia^{a,f,*} , Cátia D.F. Lopes^{a,*}

^a Institute for Bioengineering of Catalonia, Barcelona Institute of Science and Technology, Barcelona, Spain

^b Department of Biomedicine, University of Barcelona, Barcelona, Spain

^c Department of Electronics and Biomedical Engineering, Faculty of Physics, University of Barcelona, Barcelona, Spain

^d Huaxi MR Research Centre (HMRRC), West China Hospital of Sichuan University, Chengdu, China

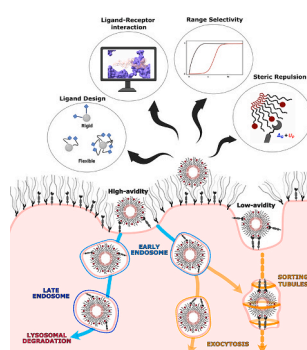
^e Department of Condensed Matter Physics, University of Barcelona, Barcelona, Spain

^f Catalan Institution for Research and Advanced Studies, Barcelona, Spain

HIGHLIGHTS

- BBB crossing remains a major obstacle for the treatment of neurological diseases.
- Multivalent systems hijack BBB transport pathways, enhancing brain targeting, transcytosis, and treatment efficacy.
- Super-selective multivalent systems reduce off-target effects and improve therapeutic outcomes in brain drug delivery.
- Combining mathematical and computational models accelerates the development of optimised brain drug delivery systems.

GRAPHICAL ABSTRACT



ARTICLE INFO

Keywords:

Blood-brain barrier
Super-selective targeting
Receptor-mediated transcytosis
Multivalency
Theoretical and computational modelling

ABSTRACT

Efficient drug delivery across the blood–brain barrier (BBB) remains a significant obstacle in treating central nervous system (CNS) disorders. This review provides an in-depth analysis of the structural and molecular mechanisms underlying BBB integrity and its functional properties. We detail the role of key cellular and molecular components that regulate selective molecular transport across the barrier, alongside a description of the current therapeutic approaches for brain drug delivery, including those leveraging receptor-mediated transcytosis. Emphasis is placed on multivalency-based strategies that enhance the specificity of nanoparticle targeting and improve transport efficacy across the BBB. Additionally, we discuss the added value of integrating

[☆] This article is part of a special issue entitled: ‘Circadian in Neuro’ published in Advanced Drug Delivery Reviews.

* Corresponding authors at: Institute for Bioengineering of Catalonia, Barcelona Institute of Science and Technology, Carrer Baldri Reixac 10–12, 08028 Barcelona, Spain.

E-mail addresses: gbattaglia@ibecbarcelona.eu (G. Battaglia), clopes@ibecbarcelona.eu (C.D.F. Lopes).

¹ These authors contributed equally.

mathematical and computational models with experimental validation for accelerating BBB-targeted delivery systems optimisation.

1. Brain barriers: Understanding the frontlines for brain drug delivery

Neurological disorders are major causes of global disability and are the second leading cause of death after cardiovascular diseases, posing significant economic and health burdens to societies worldwide [1]. The low success rate of brain therapeutics discovery is largely due to the failure of designed compounds to cross the brain barriers and reach brain targets at therapeutic doses. Paradoxically, these barriers that exclude approximately 98 % of small-molecule and nearly all large-molecule brain therapeutics are also those that safeguard the brain's integrity, promote long-term neural health and support life overall. They shield the brain from potentially toxic substances, pathogens, and

fluctuations in its chemical composition that could disrupt delicate neuronal activity and cognitive function. Brain barriers are highly selective rather than impermeable, allowing essential molecules such as glucose, oxygen, and amino acids to pass through. This selective permeability is achieved through the joint action of multiple cellular and molecular components, which prevent the free movement of most molecules and regulate what enters and leaves the brain. Therefore, by understanding the anatomy and physiological mechanisms ruling their function, one can establish more efficient, safe and targeted treatments for neurological disorders while enhancing the brain's natural protective mechanisms.

The initial evidence for the existence of a barrier between the bloodstream and the brain was documented by Paul Ehrlich in 1885. He

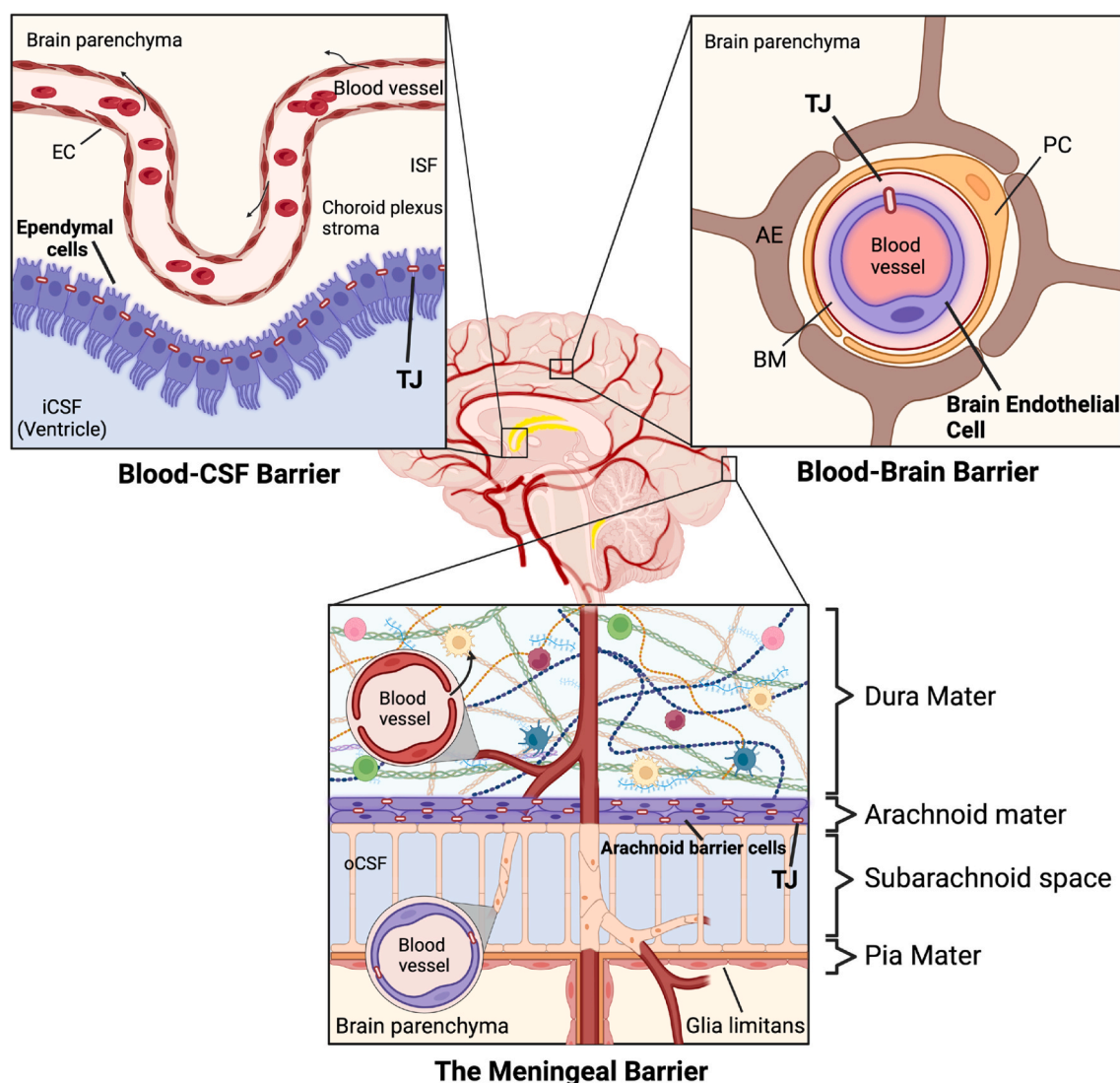


Fig. 1. The key protective barriers of the central nervous system. The blood-cerebrospinal fluid (CSF) barrier is formed by ependymal cells interconnected by tight junctions (TJ), separating the blood from the inner CSF (iCSF) in the ventricles of the choroid plexus. The blood-brain barrier (BBB), composed of brain endothelial cells (EC), pericytes (PC), astrocytic endfeet (AE), and the basal membrane (BM), tightly regulates molecular exchange between the blood and brain parenchyma through TJ and active transport mechanisms. The meningeal barrier, formed by arachnoid barrier cells connected by TJ, regulates the flow of outer CSF (oCSF) in the subarachnoid space and maintains interaction with the glia limitans adjacent to the brain parenchyma. The cells responsible for barrier properties are highlighted in purple. The interstitial fluid (ISF) has been indicated as it is found in the interstitial spaces or tissue spaces not occupied by cells. (For interpretation of the references to colour in this figure legend, the reader is referred to the web version of this article.)

noted that certain dyes, when injected into the bloodstream, failed to penetrate the brain. Ehrlich attributed his observations to the lack of affinity that these dyes had for brain tissue. Subsequently, his student, Edwin Goldman, conducted counter-experiments to demonstrate that while parenterally injected dye does not stain the brain, it does when injected into the subarachnoid space [2]. Through these experiments, Goldman demonstrated that the CNS is physiologically compartmentalised from the rest of the body. However, many authors recognise Lewandowsky as the pioneer in proposing that cerebral capillaries have specific restrictive properties with respect to some compounds [3]. With the advent of electron microscopy, Reese and Karnovsky showed for the first time that the endothelial cells of cerebral capillaries, characterised by their continuity due to the tight junctions (TJs), comprised the functional barrier [4]. Since then, the description of the brain barrier types, anatomy and physiology has progressively evolved to the current knowledge.

In the adult brain, brain barriers are found separating two primary brain interfaces: the blood-cerebrospinal fluid (CSF) and the blood–brain parenchyma interfaces. Within these regions, three main barriers have been identified, including the blood-CSF barrier at the choroid plexus of the brain ventricles, the meningeal barrier at the outer layer of the arachnoid membrane, and the blood–brain barrier (BBB), the most well-studied barrier located at the level of cerebral vessels (Fig. 1) [5,6]. The common functional player between these barriers are TJs, which form a seal between adjacent cells, restricting the paracellular passage of molecules.

The blood-CSF barrier at the choroid plexus is primarily formed by ependymal cells with unique apical TJs that inhibit paracellular diffusion of blood components into the inner CSF and adjacent brain interstitial fluid (ISF) (Fig. 1). These modified epithelial cells have a secretory function and are responsible for CSF production [7]. Active transport mechanisms on the apical surface of ependymal cells, such as the Na^+/K^+ ATPase pump, generate osmotic gradients that drive fluid formation and maintain CSF composition.

The meningeal barrier, also known as the arachnoid barrier, is formed by epithelial-like arachnoid barrier cells in the outer layer of the arachnoid membrane (Fig. 1). These cells are closely interconnected with TJs and adherens junctions (AJs), forming a barrier between the outer CSF in the subarachnoid space and the superficial dura mater, a dense collagenous membrane adjacent to the skull that contains fenestrated vasculature and lymphatic vessels. In contrast, blood vessels in the subarachnoid space are comparable to the cerebral blood vessels, presenting TJs yet lacking surrounding pericytes and astrocytic endfeet. This barrier plays a crucial role in the efflux of brain waste products, and due to the presence of pores and vesicles in the epithelium, it enables some water-soluble substances to enter the CSF [8].

The BBB is located at the level of cerebral blood vessels and regulates the exchange of substances between the blood and the brain's ISF. Considering the extensive length of the human brain's vascular network, about 644 km, and with capillaries accounting for over 85 % of the total length of cerebral blood vessels, the BBB serves as the largest interface for solute transport, estimated to be around 120 cm^2 per gram of brain tissue [9–13]. The BBB features a supracellular organisation, where a continuous non-fenestrated monolayer of brain endothelial cells (BECs) lines the cerebral capillaries. BECs are surrounded by a specialised basal lamina, pericytes, and perivascular astrocytes end feet (Fig. 1). Along with surrounding neurons, microglia, and the extracellular matrix (ECM), they form a multicellular neurovascular unit (NVU) responsible for regulating cerebral blood flow to meet local metabolic demands driven by neural activity. Consequently, the NVU is critical for supporting BBB integrity and maintaining the brain's homeostasis.

2. Barrier mechanisms at the BBB

To fulfil its barrier function, structural junction proteins (*e.g.*, TJs and AJs), along with membrane receptors, transporters, efflux pumps,

and other cellular components expressed in BECs, are fundamental to ensure barrier integrity and support brain metabolism. The sealing effect of TJs is crucial not only because it restricts the paracellular passage of even small molecules but also because it enables the coordinated action of various cellular exchange processes at the barrier interface [14]. Consequently, the transport of essential molecules (*e.g.*, metabolic substrates and nutrients) from the bloodstream to the brain, as well as the clearance of metabolic waste from the brain's ISF to the blood, is tightly regulated. For instance, carbohydrates (*e.g.*, glucose), amino acids, vitamins, hormones, nucleotides, and monocarboxylic acids (*e.g.*, lactate) are transported via solute carriers; peptides and proteins are typically transported through specific membrane receptors; and xenobiotics and drugs are often selectively transported via efflux pumps, such as adenosine triphosphate (ATP)-binding cassette (ABC) transporters [5,10]. Some of these transport systems will be explored further in this review.

2.1. Structural mechanisms

2.1.1. Glycocalyx

The BBB's first structural barrier mechanism is the endothelial glycocalyx (GCx), which is vital in preserving its integrity. The GCx is highly expressed on endothelial cells and represents a complex mesh-like network of membrane-anchored glycolipids and glycoproteins extending to the vascular lumen. In BECs, GCx operates as a unique luminal ECM that governs BBB permeability by forming an electrostatic barrier and modulates the dynamic interactions between BECs and circulating immune cells.

Proteoglycans (PGs) are a subclass of glycoproteins, with around 43 distinct members, which have carbohydrate chains (*i.e.*, glycans) in the form of glycosaminoglycans (GAGs). These are long and linear polysaccharides that typically include heparan, chondroitin, keratan and dermatan sulfate, heparin, and non-sulphated hyaluronic acid (HA) [15]. In addition to providing a net negative charge, sulfate groups increase the rigidity and polarity of GAGs, which together prevent large negatively charged molecules from the bloodstream from entering the brain. Despite the diversity of PGs, which differ in their core protein and the types of GAGs attached, the main core PG proteins are members of the syndecan and glypican families. While syndecans are membrane-spanning proteins, glypicans are covalently attached to the cell membrane via a glycosylphosphatidylinositol (GPI) anchor, making them highly mobile on the cell surface [16]. As shown by Song *et al.*, the human and mouse brain endothelium express syndecan-2, -3, and -4, as well as all six members of the glypican family (-1, -2, -3, -4, -5, and -6), with the exception of glypican-2, which is not detected on mouse brain endothelium [17].

Similar to PGs, other glycoproteins of the glycocalyx function as adhesion molecules on the surface of BECs. They comprise selectins (P- and E-) that participate in the adhesion of leukocytes immunoglobulin superfamily (*e.g.*, intercellular adhesion molecule-1, ICAM-1; vascular cell adhesion molecule-1, VCAM-1; and platelet endothelial cell adhesion molecule-1, PECAM) [18], and integrins (*e.g.*, $\alpha\text{v}\beta3$, $\alpha5\beta1$) that mediate the adhesion of platelets and linkage of ECM proteins [19].

In summary, all GCx components work together in various roles to maintain BBB integrity. This includes working as a physical and charge barrier, regulating vascular permeability, and modulating the inflammatory response, among others.

2.1.2. Brain endothelial cells

BECs line up the luminal surface of the brain's vascular system, creating a continuous and specialised cell monolayer that constitutes the barrier-forming cellular layer of the BBB [20]. In contrast to peripheral endothelial cells, BECs display a high degree of asymmetry between their luminal and abluminal surfaces (*i.e.*, polarisation), lack fenestrations, and express a thick glycocalyx. Near their luminal surface, BECs express a number of TJ proteins that extend across the lateral borders of adjacent cells and prevent the free paracellular diffusion of molecules

and entry of immune cells. By restricting the paracellular diffusion, TJs also contribute to the distinctive high transendothelial resistance (TEER) value observed at BBB [20–22]. Consequently, the TEER value generally serves as a reliable indicator of the integrity and functionality of the BBB, which typically exceeds $1,000 \Omega \cdot \text{cm}^2$ in brain endothelium within adult in vivo models. This is significantly higher than the values observed in peripheral capillaries, which range from 2 to $20 \Omega \cdot \text{cm}^2$ [23].

Polarisation plays a significant role in regulating endocytosis and directional transport in BECs. At their luminal surface, BECs typically display a low endocytic rate to prevent indiscriminate uptake of substances from the bloodstream that could be harmful to the brain. At this surface, BECs express specialised membrane proteins, including those contributing to receptor-mediated transport (RMT), ion transporters, solute carriers and efflux pumps, which restrict endocytosis for vital molecules while simultaneously facilitating the clearance of metabolic waste into the bloodstream. To sustain such ion gradients and active transport mechanisms, BECs typically feature many mitochondria to support the substantial energy requirements [24]. On the abluminal domain, the membrane is usually enriched with proteins that mediate cell-ECM interactions or provide signalling functions, for instance, to regulate TJ integrity [25]. Additionally, BECs express reduced leukocyte adhesion molecules (LAMs), limiting immune cell infiltration and immune-related brain damage [26]. These features render BECs uniquely adapted to form the BBB and precisely regulate CNS homeostasis.

2.1.3. Pericytes

Pericytes are specialised contractile mural cells embedded in the basement membrane that wraps around 70–80 % of the abluminal side of BECs in capillaries and post-capillary venules. They connect to BECs through gap and adherens junctions, allowing them to provide structural and nutritional support to BECs. Precapillary pericytes express receptors for vascular mediators such as catecholamines, angiotensin II, and vasopressin [27] and mainly control capillary blood flow by relaxing or contracting in response to signals that change intracellular calcium levels. Capillary and post-capillary pericytes are more related to BBB maintenance and immune response regulation ([28] for a review). This includes inducing the formation of TJ between BECs and regulating the permeability of ions and metabolites by secreting angiopoietin 1 [29], participating in the formation and degradation of ECM by secreting laminin, collagen IV, nidogen and perlecan, as well as metalloproteinase-2 and -9 (MMP-2 and MMP-9), contributing to vessel maturation and stabilisation by secreting the tissue inhibitor of MMP-3 (TIMP-3) [30–32], facilitating the clearance of cellular debris and harmful foreign compounds [33], and attracting circulating immune cells by secreting proinflammatory cytokines and chemokines [34,35].

2.1.4. Astrocytes

Astrocytes, the predominant glial cells in the CNS, have a star-like shape and play a diverse range of functions beyond BBB regulation. At the BBB, astrocytes extend their long branching processes to surround capillaries, making interactions with pericytes and BECs. Astrocytes provide both structural and biochemical support for BBB integrity. By expressing dystroglycan, a transmembrane glycoprotein that links the ECM to the actin cytoskeleton, astrocytes maintain their end-feet attachment to the BBB, which is critical for its structural integrity and stabilisation [36]. Similarly to pericytes, astrocytes secrete diverse factors, such as transforming growth factor-beta (TGF- β), angiopoietin 1, and MMPs, that are key in promoting TJ formation in BECs and contribute to the basal lamina formation and remodelling [37,38]. Astrocytes regulate ionic and water balance at the blood–brain interface by expressing aquaporin-4 (AQP4) water channels at their end-feet surrounding capillaries. These channels enable the transport of water across the astrocyte membrane, thereby assisting in the maintenance of osmotic balance between the blood and the brain, consequently preserving the volume of the brain's extracellular fluid and preventing edema [39].

Moreover, astrocytes help regulate extracellular pH [40] and remove metabolic waste products [41,42].

2.1.5. Basal lamina

The basal lamina, also known as the basement membrane, is a complex amorphous structure with a thickness of 50–100 nm that surrounds astrocytes, pericytes, and BECs. It comprises several ECM proteins synthesised by BECs, pericytes and astrocytes, including laminins, nidogens, heparan sulfate proteoglycans (HSPGs), collagen type IV, and other glycoproteins [43]. At the capillary level, two distinct basal lamina layers can be identified: the inner endothelial basal lamina, which is secreted by pericytes and BECs, and the outer parenchymal basal lamina produced by astrocytes and commonly referred to as the *glia limitans perivascularis* [44]. The two layers differ in the laminin isoforms composition: laminin-411 ($\alpha 4 \beta 1 \gamma 1$) and -511 ($\alpha 5 \beta 1 \gamma 1$) (mainly generated by BECs) are predominantly found in the endothelial basal lamina, while laminin-211 ($\alpha 2 \beta 1 \gamma 1$) (predominantly produced by astrocytes) is primarily found in the parenchymal basal lamina [44,45]. This differentiation ensures each basal lamina fulfils specific cellular needs: laminin-411 and -511 enhance endothelial cell function, vascular stability, and BBB permeability, while laminin-211 promotes astrocyte attachment and neuronal interactions, aiding *glia limitans* formation [46–48].

2.2. Molecular mechanisms

2.2.1. Adherens and tight junction proteins

AJs are primarily composed of cadherins (transmembrane proteins that connect adjacent cells) and catenins (intracellular proteins that bind cadherins to the cytoskeleton) [49]. Although AJs are present in all vascular beds, vascular endothelial (VE)-cadherin or CD144, neural (N)-cadherin, and cadherin-10 are the most predominant in the brain endothelium [50]. Altogether, AJs mediate strong cell–cell adhesion, contributing to the BBB formation, maintenance and regulation. For instance, VE-cadherin mediates the intracellular activation of the β -catenin pathway, which turns into claudin-5 increased expression. At the same time, N-cadherin facilitates adhesive connections between endothelial cells and pericytes, which is fundamental for sustaining BECs' function [49,51].

TJs are more abundant in the brain's endothelium than other vascular tissues, contributing to the increased sealed paracellular junctions observed at the BBB. TJs are a network of transmembrane proteins, including claudin, occludin, and junctional adhesion molecule (JAM), as well as intracellular scaffolding proteins that link these transmembrane proteins to the actin cytoskeleton [52]. Together, these proteins create a tight seal between adjacent BECs, which only allows the passive diffusion of small uncharged solutes up to a size of 5 \AA (i.e., O_2 , CO_2 , ethanol) [5]. As a result, the BBB in vivo shows a high transendothelial electrical resistance of $\sim 1800 \Omega \cdot \text{cm}^2$ [53]. Such a compact paracellular structure limits the lateral diffusion of lipids and integral membrane proteins, thereby establishing and maintaining BECs' polarity [54].

One of the key integral components of the TJ complex at the brain endothelium is the claudin transmembrane protein family. Claudins have four transmembrane domains, two extracellular loops forming a β -sheet, and an intracellular PDZ-domain at the C-terminus. The level of heterogeneity in these domains generates more than 25 classes of claudin proteins, ranging from 20 to 27 kDa, each with unique properties and functions [55]. The predominant claudin protein at the BBB is claudin-5, followed by claudin-3 and claudin-12 [56]. Specific claudin subcategories can create both homo- and heterodimers, enabling various interactions that allow for flexible and dynamic regulation of TJs. For instance, claudin-1, -3, and -5 can engage in both *cis* (within the same cell) and *trans* (between neighbouring cells) interactions, while claudin-2 and -11 are typically only found in *cis* configuration [55]. The interplay of these interactions directly affects the permeability of the endothelium where these claudins reside. For example, Nitta *et al.* studies on

claudin-5 knockout mice have shown that disrupting claudin-5 expression leads to a looser BBB and increased permeability [57]. Interestingly, *in vitro* experiments have revealed that knocking down claudin-5 reduces claudin-15 expression, while claudin-1 is significantly overexpressed [58]. Consequently, the endothelium permeability changes whilst the integrity of the TJs is preserved, which supports the idea of a complex intracellular network behind claudins. Despite the fact that claudin-3 is typically expressed at low levels in the BBB, knocking it down has been associated with reduced claudin-5 expression and increased TJ forking [55,59].

Occludin, another abundant TJ protein at the BBB, is a member of the tight junction-associated MARVEL proteins (TAMPs) family and is structurally similar to claudin [60,61]. It is primarily localised at the apical region of BECs, where it interacts with claudins and other TJ proteins. Indeed, evidence exists regarding the occludin's ability to homo- and heterodimerise through its C-terminus coiled-coil domain, indicating a possible role as a stabiliser of TJ assemblies. Phosphorylation of this domain influences complex formation with claudins and scaffolding proteins, such as zona occludens (ZO) proteins [62]. The *in vitro* co-transfection of occludin and claudin-11 in BECs showed an augmented formation of P-face-associated claudin-11 strands, supporting the hypothesis that occludin arranges TJs [58]. In the opposite scenario, vascular endothelial growth factor (VEGF)-mediated phosphorylation of occludin increases its cytoplasmic localisation in bovine retinal endothelial cells, leading to endothelium breakdown [63]. Nevertheless, studies have proposed a secondary role of occludin in TJs formation. For example, Saitou *et al.* showed that occludin-deficient embryonic stem cells present intact TJ formation and ZO-1 normal localisation and expression levels [64,65]. However, Bendriem *et al.* observed that occludin mutations can cause postnatal growth retardation and other histological abnormalities, indicating that occludin plays a role beyond TJ formation, with its dysfunction linked to various pathologies [66].

JAMs are single-spanning membrane proteins belonging to the immunoglobulin superfamily. They have one extracellular domain and a cytoplasmic tail with a PDZ domain that interacts with scaffolding proteins, such as ZO-1 [67]. JAMs maintain brain endothelial cell polarity and aid leukocyte migration [68].

Scaffolding proteins belong to the membrane-associated guanylate kinase (MAGUK) family and function as accessory elements for TJ's transmembrane components. They include ZO proteins (*i.e.*, ZO-1, ZO-2 and ZO-3), cingulin and ASIP/Par3 [69]. ZO-1 protein is the primary scaffolding protein required for BBB formation [70]. It binds to claudins, occludins and JAMs via the PDZ domains as well as to the cytoskeleton [70]. ZO proteins retain nuclear localisation and export sequences, explaining their presence in nuclei during proliferation [71]. When cell confluence is reached, they quickly redistribute to the plasma membrane [69]. This observation primarily comes from epithelium studies, but similar processes likely occur in the endothelium.

2.2.2. Efflux pumps

Efflux pumps are transport proteins embedded in membranes that actively remove specific molecules from cells. To regulate access to the brain, BECs express various efflux pumps that employ distinct mechanisms to transport molecules back into the bloodstream. The ABC transporters are multidomain integral membrane proteins that actively shuttle molecules through membranes, harnessing the energy released by ATP hydrolysis [72]. In the context of the BBB, ABC transporters prevent the accumulation of toxic metabolites in the CNS by pumping them out to the blood [73,74]. Nevertheless, this CNS protective mechanism also impacts the success of drug delivery into the brain. While the BBB naturally permits the entry of high lipophilic molecules, ABC transporters hinder the effective entry of many drugs with such properties, affecting their potential use for treating many CNS disorders [75]. Among ABC transporters, those that serve the most crucial functions at BBB encompass the multidrug resistance 1 (MDR1), commonly

referred to as P-glycoprotein (P-gp), the breast cancer resistance protein (BCRP), and the multidrug resistance-associated protein 1 and 5 (MRP1 and MRP5) [74,76].

The P-gp is a 170 kDa transmembrane glycoprotein encoded by the *MDR1* gene, classified as an ABC transporter subfamily B member 1 (ABCB1). P-gp was first identified in 1989 within human BECs and was recognised as the mechanism protecting the brain from harmful lipophilic compounds commonly present in natural sources [75]. It comprises two transmembrane domains with two intracellular nucleotide-binding domains (NBDs) with ATPase activity that regulates the transport of drugs. The ATPase activity is guaranteed by the Walker A/B motifs of one NBD and the LSGGQ (Leucine, Serine, Glycine, Glycine, Glutamine) motif of the other NBD as glutamate residues react with ATP, inducing its hydrolysis [77]. Indeed, one way to reduce the ATPase activity of P-gp is by mutating those glutamate residues, which likely trap the ABC transporter into a close and less active conformational state [78]. In 2018, Kim *et al.* revealed the outward-facing conformation of P-gp for the first time [77]. They showed the importance of ATPs and their binding site in enclosing the intracellular domains into a characteristic head-to-tail dimer, which then promotes the opening of the binding site toward the extracellular space. Interestingly, the P-gp can still transport drugs when it interacts with non-hydrolysable ATP analogue AMP-PMP, suggesting that drug release may occur before ATP hydrolysis and that the cryo-TEM structure identified in 2018 represents the post-translocation state [77]. P-gp is widely expressed in biological barriers, such as the gastrointestinal tract, kidney, liver, ovary, placenta, and BBB [79]. At the BBB, P-gp expression is localised at the apical membrane of BECs, thus managing the unidirectional efflux transport of molecules to the bloodstream for clearance [74,80]. P-gp substrates typically display amphipathic properties, often featuring aromatic groups and being uncharged or weakly basic. These traits likely align with the translocation mechanism, during which the ABC transporters integrate the substrate into the inner hemi-leaflet of the cell membrane before its release [72]. Regrettably, several anticancer drugs share these specific chemical properties, thus acting as excellent P-gp substrates with limited CNS access. These include, among others, epipodophyllotoxins, vinca alkaloids, anthracyclines, camptothecins, anthracene-dione, and heavy metal oxyanions [72,75,79]. Additionally, there is evidence that elevated P-gp expression occurs with frequent administration of its substrate [81,82]. Hence, developing P-gp inhibitors has become a common avenue for overcoming drug delivery issues to the CNS. In rodents, the P-gp expression at the BBB is encoded by the *mdr1a* gene, while its expression within the brain parenchyma (astrocytes, microglia and neurons) is regulated by the *mdr1b* gene. The significance of P-gp activity in maintaining brain homeostasis was clearly demonstrated in *mdr1a* and *mdr1b* knockout mice, in which up to a 100-fold increased sensitivity to potent toxins (P-gp substrate drugs) and consequent increased brain toxicity [80]. In addition, an upregulation of another member of the ABC transporter family was observed, the BCRP [83]. BCRP is also located at the luminal membrane of BECs, where it possibly cooperates with P-gp [84,85].

The range of molecules that can be shuttled off the brain increases due to the interplay between P-gp and MRP. MRP is a class of efflux pumps classified as ABC transporter subfamily C (ABCC) [86]. MRP share only 15 % of homology with P-gp and presents an additional transmembrane domain, which aids in discerning the cargo between the two ABC transporter subfamily [87,88]. Indeed, MRP mainly pumps organic anions and glucuronide or glutathione-conjugated compounds out of the brain [87]. MRP family presents nine different homologue pumps, MRP1-MRP9, yet only four of them, MRP1, -4, -5, and -6, have been identified by *in vitro* and capillary depletion studies at the BBB [88]. Interestingly, MRP1 typically localise at the basolateral of polarised cells, albeit it is exceptionally found together with P-gp at the apical membrane of BECs [87]. Moreover, immunolocalisation studies showed that MRP4 and MRP5 share the luminal side of BECs with MRP1 [89].

2.2.3. Endogenous transport systems

Large molecules required for brain homeostasis that cannot cross BEC's membrane via passive diffusion are transported through specific endogenous transport systems: i) carrier-mediated transport via solute carrier proteins (SLCs), ii) adsorptive-mediated transport (AMT), and iii) RMT. These transport systems can be either directional or bidirectional. Influx transporters mediate the entry of blood-borne solutes into the brain, while efflux transporters facilitate the removal of solutes from the brain to the blood [90]. Many of these processes are energy-dependent, reflecting the high metabolic demand of the brain [24].

SLCs constitute a large class of transporters, counting around 450 transporters distributed over 50 sub-families [91], and supply the CNS with ions and essential nutrients, such as glucose, amino acids, and fatty acids. They are integral membrane proteins localised on the cell surface and within organelle membranes. SLCs can function as uniporters (transporting one solute at a time), symporters (transporting two or more solutes simultaneously in the same direction), or antiporters (transporting two or more solutes in opposite directions). Moreover, SLCs include both facilitative transporters, which are energy-independent and enable solute movement following the concentration gradient (e.g., glucose transporter SLC2A1 or GLUT-1), and secondary active transporters, which are energy-dependent and transport compounds against their concentration gradient by coupling to the movement of another solute down its gradient. The former category relies on electrochemical potential differences or ion gradients generated by primary active transporters like the Na^+/K^+ ATPase, which directly uses ATP for transporting substrates across biological membranes [9].

AMT is a receptor-independent, non-specific transport mechanism based on electrostatic interactions between positively charged molecules and the negatively charged plasma membrane of BECs (i.e., glycocalyx). A common example of naturally occurring AMT is albumin modified with hexamethylenediamine (HMD), which increases its positive charge [92,93]. In the AMT, the binding affinity is low, but the binding capacity is high, and saturation is unlikely. Upon initial binding, endocytic vesicles form at the luminal surface and move through the endosomal pathways before being exocytosed into the brain parenchyma. While defined by its non-specific characteristics, some studies indicate that AMT involves caveolar endocytosis [94]. Nevertheless, AMT does not solely rely on caveolae-mediated endocytosis, as evidenced by the endocytosis of cationised Fab fragments in cells devoid of caveolae [95].

Unlike AMT, RMT is a highly specific transport mechanism based on the interaction between a substrate and its specific receptor expressed on the cell surface. In this process, the substrate binds to its receptor, forming a complex that is internalised via vesicular transport and intracellularly trafficked through various cellular compartments or across the cell (i.e., transcytosis) [46]. At the BBB, RMT primarily occurs at the luminal BEC membrane, but it can also involve the abluminal membrane, depending on the transport direction. It is an energy-dependent process, requiring ATP for both vesicle formation and trafficking. BECs usually employ this mechanism for transporting essential macromolecules needed for brain functions. Examples of molecules transported through RMT include insulin and transferrin (from blood to brain) and apolipoproteins (from brain to blood) [96]. The insulin receptor (INSR) was one of the first RMT mechanisms identified in BECs [97]. It is a single-pass type I membrane protein with a hetero-tetrameric structure and is a member of the receptor tyrosine kinase family. It is expressed in both BECs and peripheral endothelial cells. It is formed by two alpha chains, which bind insulin, and two beta chains, the tyrosine kinase domains. Upon insulin binding, INSR changes conformation, activating its intrinsic tyrosine kinase activity and triggering downstream signalling pathways. Eventually, this signalling cascade regulates glucose uptake and releases it in BECs [98,99]. The transferrin receptor (TfR) is a single-pass type II transmembrane protein abundantly expressed on the luminal side of BECs, whose primary function is to mediate iron uptake. After the transferrin-iron (Tf-Fe) complex binds to

TfR, the complex is internalised into early endosomes, and iron is released when the endosomal pH acidifies. The Tf-TfR complex is then recycled back to the cell surface, and upon returning to a neutral pH, Tf is released from the TfR [100,101]. Low-density lipoprotein receptor-related protein 1 (LRP1) is a member of the low-density lipoprotein receptor (LDLR) superfamily, which includes receptors such as LRP2 and LRP8 that share structural similarities and functional domains. LRP1 is a large transmembrane protein, approximately 600 kDa in molecular weight, expressed in both peripheral tissues and BECs. In BECs, it is localised on both the luminal and abluminal sides, with some evidence suggesting a predominance on the abluminal membrane [102]. Typically found in lipid rafts, LRP1 can migrate to clathrin-coated pits, undergoing constitutive endocytosis and recycling [103]. Its extensive extracellular domain binds various ligands, including proteases, ECM proteins, lectins, and lipoproteins such as apolipoprotein E isoforms (ApoE2 and ApoE3). By interacting with numerous ligands, LRP1 acts as a sensor of the cellular microenvironment, influencing cell physiology and signalling. Consequently, LRP1 is involved in various biological functions, including lipid transport, clearance of apoptotic or necrotic cells, modulation of cell signalling pathways, and regulation of gene expression [104,105]. It may also regulate the activity of other signalling receptors by controlling their abundance in the plasma membrane [106,107].

3. Current approaches and challenges for BBB crossing

Despite the potential of small-molecule drugs to permeate the BBB by passive diffusion, only about 2 % have been shown to reach the brain [108]. This is due to strict molecular property requirements and the activity of endogenous efflux pumps like P-gp, which limit their brain accumulation and therapeutic effectiveness [109]. A common strategy to enhance the BBB permeation of small-molecule drugs is to structurally modify them to resemble substrates of endogenous endothelial carrier proteins. This is exemplified by the anti-parkinsonian levodopa drug [110], the anti-cancer melphalan drug [111], and the anti-epileptic gabapentin drug [112], which are structurally similar to phenylalanine and are, therefore, transported by the L-type amino acid transporter 1 (LAT1). Despite improving the endothelium plasma membrane permeation of amino acid-related small drugs, these carrier-mediated systems are unsuitable for large-molecule therapeutics. For such molecules, efficient brain drug delivery requires tailored strategies that extend beyond the chemical modification of the drugs.

Large-molecule therapeutics, such as proteins and nucleic acids, face significant challenges in crossing the BBB through passive diffusion due to their size and structure. However, leveraging the endogenous transport mechanisms of BECs offers a promising avenue for enhancing brain drug delivery [96,113]. For that, large-molecule therapeutics can be either conjugated with ligands (e.g., antibodies, peptides, aptamers) specific for receptors expressed on the BEC membranes or enclosed in nanocarriers decorated with those ligands. This approach, known as the Trojan horse drug delivery strategy, has gained attention for its potential to deliver large therapeutics to the brain more efficiently. Nanocarrier-based brain drug delivery has gained particular attention for its potential for carrying water-insoluble drugs, controlling drug release and reducing systemic side effects of current therapeutics [114]. Over the past 40 years, a variety of nanocarriers have been developed for therapeutic applications in a variety of fields, including vaccine development, tissue engineering, and oncology [115]. They are generally classified into three main categories: i) polymer-based nanocarriers, including micelles, polymersomes, and dendrimers; ii) lipid-based nanocarriers, such as liposomes, solid lipid nanoparticles (SLN), and nanoemulsions; and (iii) inorganic-based nanocarriers, like gold and silica nanoparticles, as well as carbon nanotubes (CNT).

Like other cell types, BECs express a variety of receptors on their surface that play roles in one or more aspects of RMT. As a result, numerous receptor-specific antibodies, proteins, and peptides have been

Table 1

Receptor-ligand pairs exploited for enhanced brain delivery via receptor-mediated blood–brain barrier (BBB) transcytosis.

BBB Receptor	Targeting Ligand/Delivery System	Status	Key Results	Ref.
Low Density Lipoprotein Receptor 1 (LRP1)	AP2	Preclinical in vitro	Higher transport across the BBB both in vitro and through in situ brain perfusion, compared to transferrin	[169]
	ApoE4 decorated lipid NP	Preclinical in vitro and in vivo, mouse model	ApoE4 adsorption on polysorbate 80-stabilised lipid NP allows specific targeting of cerebrovascular endothelium, resulting in a 3-fold increase in brain accumulation in vivo compared to a non-functionalised lipid NP	[170]
	ANG1005, three paclitaxel molecules covalently linked to AP2	Clinical (Phase II)	ANG1005 crossed the BBB to a greater extent than paclitaxel and demonstrated clinical evidence of efficient intracranial anti-tumour activity	[171–173]
	Homogenous AP2 MAb anti-EGFR	Preclinical in vitro and in vivo, mouse model	Anti-EGFR mAb with dual-targeting functionality (for EGFR and LRP1) showed increased binding to LRP1 in vitro and improved accumulation in brain tissues and intracranial tumours in vivo compared to the anti-EGFR antibody alone	[174]
	AP2-functionalised lipid cubosomes loaded with CDDP and TMZ	Preclinical in vitro and in vivo, mouse model	AP2-NP showed higher BBB penetration and particle uptake compared to unconjugated NP in vitro, along with a 3-fold increase in brain accumulation in vivo compared to non-functionalised NP	[175]
	AP2-modified calcium arsenite-loaded liposomes (AP2–PEG–LP@CaAs)	Preclinical in vivo, mouse model	AP2–PEG–LP@CaAs demonstrated dual-targeting drug delivery to the BBB and glioma with superior BBB penetration compared to free ATO, LP@CaAs, and PEG-LP@CaAs in both in vitro and in vivo studies	[176]
Glucose transporter 1 (GLUT1)	HSA-ApoE NP	Preclinical in vivo, mouse model	NPs lacking ApoE are not taken up or retained within endothelial cells, likely accumulating in the lysosomal compartment. In contrast, HSA-ApoE-conjugated NPs exhibited higher uptake by endothelial cells and enhanced transport into the brain parenchyma	[177]
	Surface-modified liposomes with mannose and cell penetrating peptides (penetratin or RVG)	Preclinical in vitro and in vivo, mouse model	Functionalized liposomes demonstrated a 50 % higher transport and transfection efficiency of the BDNF gene in vitro compared to unmodified liposomes, along with a 7 % increase in BBB transport in vivo	[178]
Transferrin receptor (TfR)	Bispecific anti-TfR and anti-BACE1 antibody	Preclinical in vivo, mouse and monkey model	Anti-TfR/BACE1 bispecific antibody exhibited higher brain uptake, brain distribution and amyloid β clearance compared to anti-BACE1 or anti-TfR	[124,125,179,180]
	Branched THRre peptide	Preclinical in vitro	GFP modified with branched THRre peptide showed higher internalisation and transport in cell-based BBB cellular models by 2.6-fold compared to naked or THRre-modified GFP	[181]
	BBB-penetrating fusion protein JR-141 consisting in anti-human TfR antibody and intact human IDS	Clinical (Phase II completed, phase III ongoing)	Efficient BBB crossing with amelioration of neurocognitive and motor symptoms in patients affected by Hunter Syndrome	[182,183]
	ATV fused to BACE1 Fabs with an engineered Fc fragment	Preclinical in vivo, mouse and monkey model	ATV:BACE1 variants yielded about 10- to 40-fold higher brain IgG concentrations in rodents and > 30-fold higher IgG concentrations in cynomolgus monkeys compared to a standard anti-BACE1	[184]
	DNL310, lysosomal ETV containing IDS (ETV:IDS) fused to an Fc domain engineered to bind TfR.	Clinical (Phase II/III, ongoing)	ETV:IDS showed increased brain uptake, BBB crossing and brain distribution compared to Fc:IDS, IgG:IDS in MPS II rodents and showed improvement or stabilisation of clinical symptoms	[185–187]
	OX26, anti-TfR antibody	Preclinical in vitro	OX26 showed higher in vitro transcytosis compared to the control IgG, NiP228	[188]
	Chimeric MAb anti-TfR IgG fused to SGSH (cTfRMAB-SGSH)	Preclinical in vivo, mouse model	Null mice for the SGSH enzyme showed a 70 % reduction of HS after cTfRMAB-SGSH treatment compared to cTfRMAB alone	[189]
Insulin-like growth factor-1 receptor (IGF1R)	Single domain antibody fused to mouse Fc (SdAb-mFc) anti-IGF1R	Preclinical in vitro and in vivo, rat model	SdAb-mFc targeting IGF1R demonstrated superior BBB crossing compared to OX26, a known anti-TfR monoclonal antibody, and facilitated the transport of galanin, which does not cross the BBB on its own.	[190]
Solute carrier CD98 heavy chain (CD98hc)	Heterodimerised bispecific anti-CD98hc/BACE1 antibody	Preclinical in vivo, mouse model	Increased brain uptake of anti-CD98hc/BACE1 compared to control IgG	[191]
Basigin	Basigin mAbs	Preclinical in vitro	Basigin MABs showed internalisation and transcytosis across the brain endothelial monolayer, along with uptake by co-cultured astrocytes	[192]
Insulin receptor (IR)	Valanafusp alpha, HIRMAb-IDUA	Clinical (Phase II)	Valanafusp alpha can cross the BBB as suggested by cognitive and somatic stabilisation of patients involved in the study affected by MPS I	[193,194]
	HIRMAb-IDS	Preclinical in vivo, monkey model	HIRMAb-IDS fusion protein traversed the BBB and penetrated the brain parenchyma showing high brain volume of distribution in the post-vascular supernatant compared to the vascular pellet	[195,196]
	HIRMAb-EPO	Preclinical in vivo, monkey model	HIRMAb-EPO fusion protein crossed the BBB, resulting in increased brain EPO levels at low systemic doses, unlike free EPO, which did not cross the BBB	[119]
Diphtheria toxin receptor (DTR)	CRM197-grafted PBCA NP	Preclinical in vitro and in vivo, mouse model	CRM197/PBCA NP loaded with drugs (e.g., AZT) crossed the BBB achieving pharmacological effect without impacting BBB integrity	[197]

Abbreviations

AP2, angiopep-2; MAb, monoclonal antibody; EGFR, epidermal growth factor receptor; CDDP, cisplatin; TMZ, temozolomide; NP, nanoparticle; PEG, poly(ethylene glycol); ATO, arsenic trioxide; HSA, human serum albumin; ApoE, apolipoprotein E; RVG, rabies virus glycoprotein; BDNF, brain-derived neurotrophic factor; GFP, green fluorescent protein; ATV, antibody transport vehicle; IgG, immunoglobulin G; ETV, enzyme transport vehicle; MPS, mucopolysaccharidosis; SGSH, N-sulfo-glucosamine sulfohydrolase; HS, heparan sulfate; HIRMAb, monoclonal antibody against the human insulin receptor; IDUA, α -L-iduronidase; IDS, iduronate-2-sulfatase; EPO, erythropoietin, CRM197, crossreacting material 197 (a non-toxic mutant protein of diphtheria toxin); PBCA, polybutylcyanoacrylate; AZT, zidovudine.

explored as active ligands for targeting BECs in developing BBB shuttles. Both in vitro and in vivo preclinical studies have shown the promise of these approaches to enhance the delivery of therapeutics to the brain. (Table 1 for a summary).

As described by Pardridge and colleagues in 1987, the INSR was the first endogenous BEC receptor identified and studied, making insulin the first Trojan horse explored for brain delivery [116]. In this pioneering study, a chimeric peptide was synthesised by conjugating somatostatin, a hydrophilic peptide, to insulin, enabling it to cross the BBB via RMT. While this study laid the foundation for using BBB targeting ligands, the application of insulin as a targeting moiety was shown to be limited by the widespread expression of INSR in peripheral tissues that potentiate off-target delivery and potential side effects [97,99,117]. To circumvent this limitation, alternative strategies involving nanocarriers were developed. For instance, Dieu *et al.* designed polymersomes composed of poly(dimethylsiloxane)-block-poly(2-methyl-2-oxazoline) (PDMS-*b*-PMOXA) amphiphilic diblock copolymer functionalised with monoclonal antibodies (MAb) against the anti-human insulin receptor for active targeting of BECs [118]. The binding and uptake of these nanocarriers to a human BBB model, based on hCMEC/D3 cells expressing the human INSR, were assessed through competitive inhibition studies, corroborating their specificity for these cells. In another study, the human erythropoietin (EPO) protein was fused to the Fc (fragment crystallizable) region of an anti-INSR IgG antibody (INSRMAB) to facilitate brain delivery. Upon intravenous injection, the INSRMAB successfully shuttled EPO across the BBB via RMT, producing specific pharmacological effects in the brain while minimising activity in peripheral organs [119].

A similar strategy has been employed for targeting the brain endothelial LRP1 receptor. Gao *et al.* developed a dual-modified nanocarrier (AnACNPs) simultaneously incorporating angiopep-2 (AP2) and an activatable cell-penetrating peptide (ACP) to deliver the chemotherapeutic agent docetaxel specifically to glioma cells [120]. In this approach, AP2 targets LRP1 receptors on BECs and glioma cells, enhancing both BBB penetration and tumour drug delivery. Meanwhile, the ACP facilitated deeper tissue penetration within the tumour micro-environment. This study demonstrated that AnACNP nanocarriers effectively crossed the BBB with increased uptake and accumulation in glioma cells, exhibiting anti-tumour effects in both in vitro and in vivo models. In two independent studies, Sakamoto *et al.* explored the phage display technology to identify and develop novel peptides targeting the LRP1 receptor [121,122]. They found two new peptides, L57 and KS-487, that were shown to facilitate BBB penetration successfully under both in vitro and in vivo conditions.

Another example of a receptor explored for BBB targeting and crossing is the TfR. In a recent study, Brody and colleagues employed a mouse TfR binding nanobody, *i.e.*, small recombinant proteins derived from the binding domains of heavy chains of camelids antibodies, to mediate BBB transcytosis via RMT [123]. The TfR binding nanobody was engineered with three histidine mutations to confer pH-dependent unbinding at pH 5.5 and binding at pH 7.4, which was conjugated with neurotensin for in vivo functional testing of BBB transcytosis via central neurotensin-mediated hypothermia in wild-type mice. The authors reported a 60 % retention of such constructs in capillary depleted brain lysates at 8 h post-administration and propose this system as a useful tool for fast and efficient BBB shuttling. Similarly, Watts *et al.* developed a bi-specific antibody (bsAb), with one arm targeting the TfR and the other targeting β -secretase, a therapeutic target for AD. Their study demonstrated the bsAb brain delivery after intravenous

administration, which reduced amyloid-beta ($A\beta$) levels in both the CSF and brain tissue, with efficacy shown in both in vitro and in vivo models [124,125]. Additionally, Tf protein has also been used as a Trojan horse for nanoparticle delivery across the BBB. However, endogenous Tf present in the plasma, which is approximately 1000-fold higher than the amount of TfR in the BBB, compete for binding to the TfR, resulting in near-total receptor saturation (>99.9 %) [126]. This significantly restricts the capacity of exogenous Tf to enhance brain drug delivery.

Beyond the commonly targeted receptors described above, several other receptors have been explored to enhance drug delivery across the BBB. Examples include basigin (or CD147) [127], other LDLR family members [103,128] or leptin receptors [129], among others. These alternative receptors expand the possible ligands for RMT-based brain drug delivery strategies.

Despite these preclinical successes, often regarded as magic bullets for targeting the brain, none have been translated into clinical applications. One key contributing factor pertains to the propensity for off-target delivery. In an idealistic view of active BBB targeting, the developed Trojan horse strategies are exclusively tailored to the target cell, *i.e.*, brain endothelial cells. For this ideal concept to hold true, BECs would have to express a unique receptor that is absent in peripheral endothelial cells. However, at the cellular level, these common targets are not solely expressed in BECs but also in peripheral endothelial cells. For example, LRP1 and TfR are also found in the peripheral endothelial cells besides being overexpressed in BECs [130]. Consequently, off-target effects are likely to occur. Thus, the current challenge is to design and predict super-selective BEC nanomedicines that can not only transport therapeutics across the BBB but also discriminate and bind almost exclusively to BECs, sparing peripheral endothelial cells. This can be achieved through the multivalent effect, a central principle of super-selective targeting that will be described in the following section.

4. Super-selective BBB targeting: Theoretical and computational modelling

4.1. Multivalency for super-selective BEC targeting

Multivalency refers to the presence of multiple functional groups or ligands on the surface of a construct, such as a nanoparticle. These functional groups may be identical (homo-valent) or distinct (hetero-valent), allowing simultaneous interaction with multiple receptors on the surface of a target cell. Multivalent binding enhances the likelihood of receptor engagement by increasing the local concentration of ligands, which can lead to stronger and more selective binding compared to monovalent interactions (single ligand-receptor binding). This increased specificity and stability of multivalent binding arise from a combination of enthalpic contributions (due to stronger overall binding energy) and entropic effects (related to the reduction in the degrees of freedom upon complex formation). These contributions are explained by the thermodynamics model of multivalent binding.

In the thermodynamics of multivalent binding, both enthalpy (ΔH) and entropy (ΔS) play critical roles in determining the overall Gibbs free energy (ΔG) of the multiple and simultaneous ligand-receptor interactions. In a multivalent system, the sum of these interactions can result in a much stronger binding affinity than would be observed in a monovalent system. This cumulative effect enhances the stability of the ligand-receptor complex. The change in energy during ligand-receptor bond formation or bond breaking is defined as enthalpy. In

multivalent binding, the freedom of movement of the ligands (*i.e.*, entropy) is generally reduced due to the conformational constraints imposed on the ligands and receptors. Therefore, multivalent binding is cooperative, where the binding of one ligand influences the binding affinity of subsequent ligands. This cooperative effect in multivalent systems, which is described by the Langmuir-Hill adsorption model, can further enhance binding affinity and selectivity.

The Langmuir-Hill adsorption model is a foundational theory to describe the complex binding scenario in multivalent interactions. Assuming cell surfaces have independent adsorption sites, each capable of binding ligands in a multivalent nanoparticle, the cell surface coverage (θ), or the fraction of occupied binding sites (ligand-receptor), can be mathematically expressed as:

$$\theta = \left\langle \frac{aQ}{1 + aQ} \right\rangle$$

Here, a is the nanoparticle activity approximated by $a = [P]N_A v_B$, which combines the nanoparticle molar concentration ($[P]$), Avogadro's number (N_A), and the ligand exploration volume (v_B) to effectively capture the concentration and availability of ligands in the nanoparticle [131]. Q represents the partition function that quantifies the number of available binding states for the interaction and the associated energy distribution in the binding process, including whether a ligand is free or bound to a receptor. This partition function $Q = (N_L, N_R, \beta\Delta G)$ is defined as a function of ligand number (N_L), receptor number (N_R), and strength of ligand-receptor bond ($\beta\Delta G$), where $\beta = \frac{1}{kT}$, k denotes the Boltzmann's constant and T the absolute temperature. The $\langle \rangle$ notation indicates an averaging for Poisson distribution over different possible states of the system, suggesting that the system is considered in equilibrium with respect to both ligand concentration and binding configurations.

Therefore, this equation models the cooperative nature of multivalent binding by determining the likelihood of receptor occupancy, given a defined ligand concentration. As aQ increases due to the higher availability of ligands in the nanoparticle or due to more favourable binding conformations available, the fraction of occupied binding sites increases towards saturation (*i.e.*, complete site occupancy, $\theta=1$). However, this rise is not linear – it follows a sigmoidal curve, characteristic of cooperative systems: no binding occurs below a critical receptor density, but as the receptor density surpasses this threshold, the binding fraction sharply increases until reaching saturation (Fig. 2a). This is the basis of range selectivity. In biological applications, range selectivity can be employed to design super-selective nanomedicines that discriminate differences in cell receptor density and selectively bind

to cells expressing receptors above a specified threshold. For instance, in the context of brain drug delivery, nanomedicines can be engineered with ligands specific to receptors overexpressed on BECs. The high receptor density on BECs allows multivalent nanomedicines to bind effectively, ensuring they are delivered primarily to the BBB. However, super-selectivity in multivalent nanoparticles is typically achieved using weak binding affinity ligands. These ligands facilitate cooperative binding, where multiple weak interactions cumulatively result in strong and selective binding only when the receptor density surpasses a critical threshold. Strong binding ligands would reduce this sensitivity, as they might bind effectively even at low receptor densities, thereby decreasing selectivity (Fig. 2b).

4.2. Other critical parameters for super-selectivity

As previously noted, super-selectivity refers to the ability of multivalent systems to distinguish between target and non-target cells with exceptional precision, driven by a cooperative binding mechanism that amplifies selectivity beyond what is achievable with monovalent interactions. Building upon the foundational understanding of multivalency, where multiple low-affinity ligands work synergistically to achieve high overall binding strength, it is essential to consider additional parameters that can further enhance the super-selectivity of multivalent nanoparticles. In this section, we will briefly describe the main factors that significantly contribute to optimising super-selectivity, including multiplexing, spatial arrangement of ligands on the nanoparticle surface, and steric repulsion forces in the modulation of overall system avidity.

4.2.1. Multiplexing

Nanoparticle super-selectivity can be further enhanced through multiplexing, wherein hetero-valent ligands are concurrently incorporated into the system. Cells typically have a variety of receptor types, each having a distinct average density on the cell surface, creating a specific receptor “profile”. By selecting and using the right combination of receptors, multiplexing favours the interaction with a defined “cell receptor profile” more effectively. In our previous studies, we demonstrated the potential of multiplexed binding to discriminate between BECs and macrophages *in vitro* [132]. Polymeric nanoparticles were functionalised with two ligands: poly(2-methacryloyloxyethyl phosphorylcholine) (PMPC), which targets the scavenger receptor B1 (SRB1), and AP2, a well-established ligand for the LRP1 receptor. Experimental results revealed that nanoparticles functionalised with PMPC predominantly bound to macrophages, while those functionalised with AP2

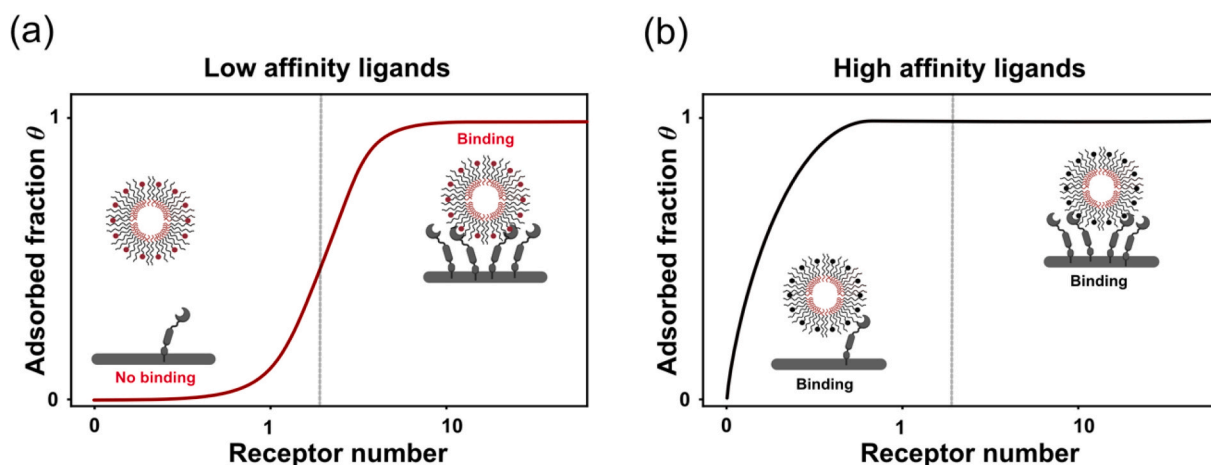


Fig. 2. Multivalent binding adsorption curves. (a) Schematic illustration depicting the adsorption fraction behaviour of multivalent nanoparticles bearing low-affinity ligands. These nanoparticles exhibit a nonlinear increase in the adsorption fraction, achieving saturation at higher receptor densities. The use of low-affinity ligands enables differentiation between low and high receptor density regimes, thereby enhancing super-selective targeting. (b) Multivalent nanoparticles with high-affinity ligands require reduced densities of the receptors to saturate, reducing selectivity.

preferentially interacted with BECs. Notably, when both PMPC and AP2 were incorporated into the same nanoparticle, a synergistic effect was observed. The binding of these dual-functionalised nanoparticles reached saturation with fewer ligands than those functionalised with a single ligand. This synergistic effect can be attributed to the differential expression levels of LRP1 and SRB1 in BECs and macrophages, enabling enhanced selectivity and binding efficiency. The described strategy can be defined as phenotypic association theory (PAT), which provides a framework for designing super-selective nanocarriers capable of improving targeting specificity based on specific cell phenotypes [133,134]. However, as previously mentioned, to achieve super-selectivity, PAT relies on low-affinity ligands.

4.2.2. Spatial arrangements

The overall binding strength (avidity) of ligand-receptor interactions is determined by a complex interplay of valency, affinity of individual binding sites, and the spatial arrangement for ligand-receptor binding (topology). For instance, more flexible ligands and receptors increase the number of possible binding configurations, thereby enhancing the overall binding probability. In opposition, with short and rigid ligands and receptors, each ligand or receptor may be independently bound or unbound to its nearest partner, decreasing the overall binding probability.

The avidity entropy, which describes the variability and distribution of binding interactions between ligands and receptors, is a nonlinear function influenced by the degeneracy of ligand-receptor pair combinations. Degeneracy, in this context, refers to the number of distinct ways in which a given number of ligand-receptor bonds (λ) can form. This is quantified by the number of bound states (Ω_λ), where λ is the number of bonds. The binding behaviour is defined by the topology of interactions, and there are three primary binding topologies:

- Indifferent topology:** in this scenario, each ligand-receptor pair binds independently, resulting in only one bound form. The degeneracy is simply the product of the total numbers of ligands and receptors, given by ($\Omega_\lambda = N_L N_R$), where (N_L) is the number of ligands and (N_R) is the number of receptors
- Linear topology:** ligands and receptors bind sequentially in a chain-like manner. The degeneracy, or the number of ways to arrange the ligand-receptor bonds, decreases as more bonds form. The number of bound states is described by $\Omega_\lambda = (N_L - \lambda + 1)(N_R - \lambda + 1)$.
- Radial topology:** in this configuration, the ligand can flexibly bind to any receptor, leading to a high degree of degeneracy. The number of possible bound states is expressed using the multinomial coefficient:
$$\Omega_\lambda = \frac{N_L! N_R!}{(N_L - \lambda)! (N_R - \lambda)!} \lambda!$$

In each topology, avidity entropy reflects the overall stability and variability of the binding interactions, highlighting how changes in spatial arrangement can significantly influence the dynamics of ligand-receptor binding. The role of topology in modulating the interaction dynamics between multivalent particles and receptors was further demonstrated by Hale *et al.* They used DNA as a ligand to construct DNA-origami disks with identical ligand valency and composition but distinct geometric arrangements [135]. Their findings revealed that by simply altering the binding topology through varying ligand geometric patterns, they could differentiate receptor interactions between constructs.

4.2.3. Avidity optimisation

Enhancing selectivity often involves a delicate balance between specific and non-specific interactions. These non-specific interactions encompass additional forces between the multivalent nanoparticle and its target that extend beyond the intended multivalent design. These may include structural interactions between the nanoparticle and the target, ligand and receptor cross-talk with other membrane molecules, as well as charge-based attractions, repulsions, and steric hindrances.

One major biological factor influencing nanoparticle avidity and selectivity is the formation of the “protein corona”, a dynamic layer of biomolecules that adsorbs onto the nanoparticle surface upon exposure to biological fluids. This phenomenon confers a new biological identity to the multivalent system, significantly altering its physicochemical properties and influencing ligand accessibility, receptor binding, and overall biological fate. These effects extend to critical processes such as bio-distribution, cellular internalisation, intracellular trafficking, and nanoparticle processing. As demonstrated by Vilanova *et al.* [136], who combined experimental approaches, simulations and mathematical modelling, the kinetics of protein-nanoparticle corona formation are governed by competitive adsorption dynamics, where the continuous associations and dissociations of adsorbed proteins establish a dynamic equilibrium that evolves over time. This constant reshaping of the corona introduces an additional layer of complexity to multivalent interactions, as the fluctuating physicochemical properties can strongly impact ligand-receptor binding efficiency. Furthermore, in the context of the BBB crossing, Cox *et al.* showed that the protein corona undergoes significant transformations during translocation across the barrier [137]. Specific proteins are selectively retained or exchanged, ultimately influencing nanoparticle transport and its overall fate, emphasising the role of the protein corona in defining nanoparticle-cell interactions. While many of these interactions are typically seen as unintended side effects of multivalent nanoparticle design, their role in enhancing targeting selectivity should not be underestimated. By understanding and controlling these forces, researchers can tailor nanoparticles to achieve a higher degree of super-selectivity.

One example of improved selectivity involves the introduction of a shielding brush into the surfaces of multivalent nanoparticles. The brush, often made of polymers like poly(ethylene glycol) (PEG), creates a steric barrier that prevents unintended interactions and ensures only target molecules can access the binding sites. As a result, the multivalent nanoparticle becomes less likely to bind non-specifically, making it more selective through better ligand orientation and increased local concentration. This concept has been effectively demonstrated by Shihu *et al.* [138], who demonstrated that a longer nonfunctional tether distribution on the nanoparticles, which permits shielding ligands, leads to extra entropy loss at the adsorption onset, enhancing the selectivity. In the specific case of polymeric nanoparticles, polymer tethers are employed to shield the ligands. As nanoparticles approach their target receptors, they experience repulsion from the polymer brush surrounding the ligands (Fig. 3). This repulsive steric, denoted as U_p , arises from the steric effects generated by the polymer chains, which create a physical barrier as a receptor is inserted inside the polymer brush. This steric is composed of osmotic pressure due to the receptor volume depleted by the polymer brush and elastic component raised from compression [139]. The extent of repulsion experienced by the receptor increases as the ligand is more deeply embedded within the polymer brush.

According to the theoretical work of Halperin, U_p can be expressed as:

$$\beta U_p = \frac{V_R (1 - \delta_p^2)^{\frac{9}{4}}}{\sigma_p^{\frac{3}{2}}},$$

where V_R represents the receptor volume, δ_p the interference parameter, and σ_p the area per polymer chain [139]. The interference parameter, δ_p , is defined as the ratio of the ligand tether length to the protected tether length [132]. According to the model proposed by Zhulina *et al.*, the σ_p is a function of the interference parameter and is mathematically described as:

$$\sigma_p = \sigma_0 \left(1 + \frac{\delta_p h_p}{R} \right)^{r-1}$$

where h_p is the height of the ligand, R is the radius of the nanoparticle,

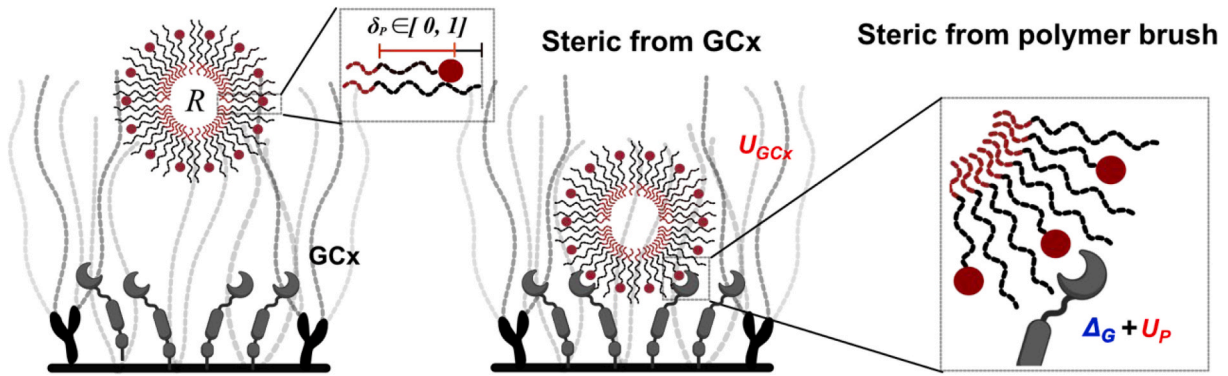


Fig. 3. Steric effects in nanoparticle-receptor interaction. Illustration of the steric repulsion forces present during nanoparticle and cell surface receptors approaching. Two sources of repulsion counteract the attractive ligand-receptor affinity: repulsion from the cell glycocalyx (U_{GCx}) and nanoparticle shielding brush steric at the single-molecule level ($\Delta G + U_p$).

and γ is the geometry parameter [140]. The density of the polymer brush is affected by factors such as the stretch of the polymer brush, the interaction of the chains, and the curvature of the nanoparticles. Longer chains will occupy more space. Larger nanoparticles will result in less curvature. These factors would indicate a larger polymer chain density. Considering the steric interference, the partition function can be reformulated to incorporate these effects:

$$Q = \sum_{\lambda=1}^{\min(N_L, N_R)} \Omega_{\lambda} e^{-\lambda\beta(\Delta G + U_p)}.$$

This partition function reflects the impact of steric hindrance imposed by the polymer brush and provides a quantitative framework for understanding how steric effects influence binding affinity and selectivity in nanoparticle-receptor interaction.

Another critical repulsive factor influencing nanoparticle-cell interactions is the GCx (Fig. 3). As described in previous sections, BECs exhibit a thick and complex GCx layer with an inherent steric repulsion effect that can be considered to improve nanoparticle engagement with the target. The steric repulsion originating from the GCx, denoted here as U_{GCx} , arises from two primary components: the osmotic pressure due to volume exclusion and the elastic force caused by the compression of the sugar chains, which is analogous to the repulsive steric as the receptor inserts into nanoparticle polymer brush [139]. Notably, when the nanoparticle radius is smaller than the GCx height, the elastic component can be considered negligible. Similar to the above mentioned model from Halperin used to describe receptor penetration into a polymer brush and focusing solely on osmotic pressure, the steric repulsion due to the GCx can be expressed as:

$$\beta U_{GCx} = \frac{V_{NP}(1 - \delta_{GCx})^{\frac{9}{4}}}{\sigma_{GCx}^{\frac{3}{2}}},$$

where V_{NP} represents the nanoparticle volume, σ_{GCx} denotes the area per GCx, and δ_{GCx} is the interference parameter related to the relative height between the receptor and the GCx [139]. Incorporating these factors, the partition function can be expressed as:

$$Q = \left(\sum_{\lambda=1}^{\min(N_L, N_R)} \Omega_{\lambda} e^{-\lambda\beta(\Delta G + U_p)} \right) e^{-\beta U_{GCx}}.$$

As described here, the collective steric effects occurring when a nanoparticle approaches the cell surface (one from the shielding brush and the other from the cell GCx) influence the total avidity of the system and, therefore, the overall interaction dynamics. Notably, cells with higher receptor density often exhibit increased GCx density. By strategically considering such steric factors, nanoparticles can be engineered for range selectivity, targeting cells within specific receptor expression

levels (i.e., super-selectivity). This dual control mechanism contributes to a better match of the ligand profile with the receptor profile on the cell surface, enhancing targeting precision.

An additional advantage of controlling the overall avidity of the system is the ability to influence the outcome of receptor-mediated endocytosis, a critical process for effective BBB crossing. While increased ligand number generally enhances binding affinity, the observed non-monotonic trend arises due to steric hindrance from unbound ligands (Fig. 4b). As the ligand density increases, unbound ligands introduce additional steric repulsion, which can partially obstruct receptor accessibility and reduce overall binding efficiency. This effect leads to a deviation from the expected monotonic increase in binding energy. Cumulative evidence shows that avidity – defined as the cumulative binding strength of multivalent interactions – can determine the intercellular fate of the nanoparticle (Fig. 4). For instance, high avidity enhances the uptake of the nanoparticle via the classical endocytic pathway, which is associated with intracellular degradation at lysosomes. Instead, moderate avidity enhances receptor clustering and internalisation via tubule-like endocytic structures, improving nanoparticle transcytosis, which is beneficial for delivering cargo to the brain. Building on these insights, Villaseñor *et al.* investigated the influence of cargo avidity on intracellular sorting at the BBB using Brain Shuttle constructs [141]. These constructs were engineered by fusing a single-chain Fab fragment derived from an anti-TfR monoclonal antibody with either one or two C-terminal ends from a distinct antibody, producing monovalent or bivalent constructs. These configurations represent two levels of cargo avidity. Monovalent constructs, characterised by lower avidity, activated transcytosis pathways at the BBB, evidenced by the formation of intracellular tubules. In contrast, high-avidity bivalent constructs were predominantly directed toward degradation pathways [141]. A similar phenomenon was reported by Tian *et al.* for AP2-functionalised polymersomes, where the number of ligands on the nanoparticle surface determined cargo avidity [142]. They have shown that the efficiency of BBB crossing does not increase linearly with the number of ligands. Instead, there is an optimal ligand density at which transcytosis is most effective. Both lower and higher ligand densities resulted in significantly reduced crossing efficiency. Notably, polymersomes with higher ligand densities, mimicking high-avidity cargo, were primarily routed through endocytic pathways associated with degradation. This can be explained by the increased ligand-receptor binding energy, which decreases the probability of nanoparticle detachment from the receptor during the unbinding process, thereby reducing the efficiency of the transcytosis pathway. These findings underscore the critical role of avidity optimisation in designing nanocarriers for effective BBB transcytosis, highlighting the need to balance binding strength and the dynamic requirements of intracellular trafficking.

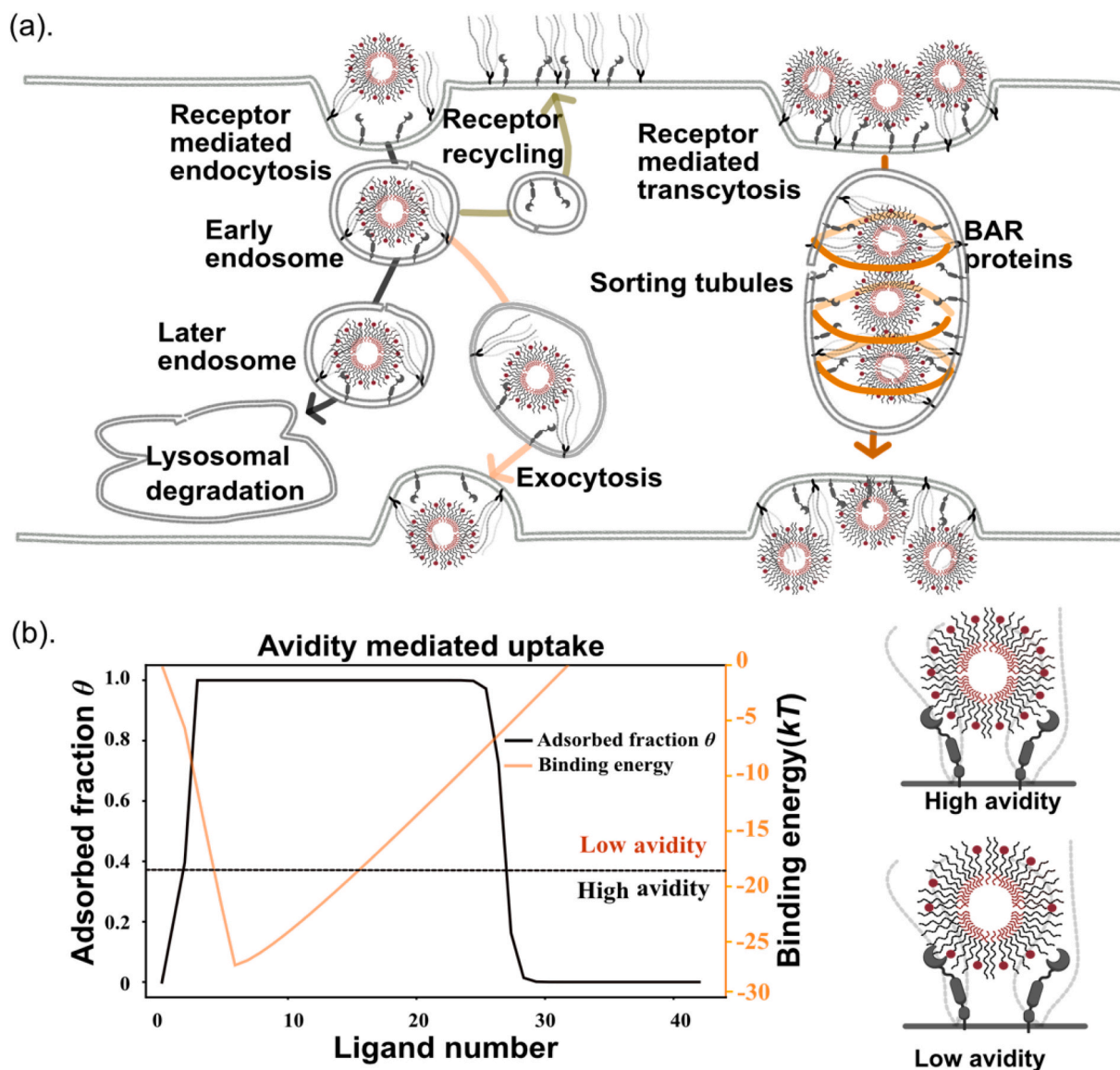


Fig. 4. Avidity-related nanoparticle uptake and intracellular trafficking. (a) Schematic representation of the impact of cumulative binding strength of multivalent interactions (avidity) on receptor-mediated endocytosis and intracellular fate of multivalent nanoparticles. High-avidity nanoparticles are more prone to follow intracellular degradation pathways after endocytosis, while low-avidity nanoparticles aggregate and undergo transcytosis across the cell. (b) Graph summarising the relationship between ligand number, adsorbed fraction, and binding energy for low and high avidity systems.

4.3. Integrated models and simulations on multivalent binding

As the computing cost of quantifying receptor-ligand interactions reduced considerably the cost of in vitro and in vivo experiments, the computational approach gained importance in years. Computational methods can aid in designing multivalent systems by providing insights about ligand-receptor interactions at atomic and molecular levels, which are difficult to achieve experimentally. Techniques such as molecular mechanics simulations, course-grain methods and molecular docking allow researchers to predict how ligands bind to receptors, estimate binding affinities, and explore the structural dynamics of complexes [143–146]. For instance, computational methods can help elucidate the structural and energetic factors governing binding, offering a deeper understanding of how Gibbs free energy (ΔG) relates to the spontaneity and stability of protein–ligand complexes. Moreover, computational approaches enable high-throughput screening of large compound libraries, such as potential ligands, significantly accelerating drug discovery processes [147,148]. By integrating computational models with experimental data, researchers can better understand the mechanisms of

ligand-receptor interactions, optimise drug candidates, and reduce the costs and time associated with experimental studies.

From a computational perspective, the multivalency theory can be considered a bottom-up theory as it relies on a set of parameters describing in detail individual ligand-receptor binding properties that, when integrated, allow the prediction of system-wide outcomes. In this sense, computational models can be applied at two key levels: first, to understand the structures of the interacting objects, such as ligands and receptors; second, to study the interactions between these objects. The object structures are typically obtained through experimental techniques like X-ray crystallography, electron microscopy, and nuclear magnetic resonance (NMR) spectroscopy, which can reveal details at the nanoscale. However, these techniques rely on the availability of biological entities, which need to be produced in vitro or extracted from living organisms. To overcome the limitations of experimental methods, predictive computational approaches like comparative homology modelling (CHM) have been developed. CHM typically uses the structure of one or more known proteins (the template) to predict the structure of an unknown but related protein (the target). These

predictions are based on high sequence homology between the template and the target. The field of protein structure prediction has been transformed by artificial intelligence, particularly with the development of deep learning models like RoseTTAFold [149] and AlphaFold2 (2024 Chemistry Nobel Prize award) [150]. These neural networks can accurately predict protein structures by recognising patterns in known primary, secondary, and tertiary structures and applying them to unknown proteins.

When the object's structure is known, computational modelling can be of added value in studying specific features of the object interactions. In this context, ligand-receptor interactions have been studied in the larger context of molecular recognition, where the non-covalent interactions mediating the formation of supramolecular complexes are investigated. In this domain, the actions of two BBB receptors were described: the ISNR and a member of the glucose transporter family, GLUT1. Using the interactive molecular dynamics flexible fitting (iMDFF) implemented in Visual Molecular Dynamics (VMD) [151], Croll and colleagues investigated the structural transitions of ISNR upon ligand binding. Their work provided a revised structure of the receptor, including missing residues, that place constraints on the receptor's conformational flexibility and, thus, on possible signal transduction mechanisms [152]. Park's work on the GLUT1 transporter ranges from modelling the protein homology using MODELLER [153] to a series of classical and accelerated molecular dynamics techniques that shed light on the mechanism of binding and release of glucose across a cell membrane, also defining the critical amino acids involved in the process [154]. In another example, Indrakumar and colleagues investigated, through molecular dynamics simulations, the conformational stability of human serum Tf at varying pH values and salt and excipient concentrations [153]. Their study provides a detailed molecular understanding of how these physicochemical conditions affect Tf protein surface properties and conformational stability, which can be utilised in designing preventive measures of aggregation in optimising Tf-mediated formulations. At the level of multivalent systems, Shityakov *et al.* benefit from the potential of molecular dynamics simulations to model, along with experimental characterisation, the potential of multi-walled carbon nanotubes as a BBB-permeating drug delivery vector, determining that the minimisation of the vdW interactions drives the aggregation kinetics [155]. Recent advancements in deep learning models, such as AlphaFold-Multimer and AlphaFold3 [156], extend the capability to predict the structures of protein complexes. Using AlphaFold-Multimer, Shay and colleagues generated capsid-receptor binding models to predict the affinity of several adeno-associated virus (AAV) for BBB receptors. They identified two key targets, LY6C1 and CA-IV, that allow them to design an enhanced LY6C1-binding vector (AAV-Ph.C.) to penetrate the BBB and deliver therapeutic drugs [157].

While molecular mechanics methods offer valuable insights into biological systems, they are constrained by the limited timescales and system sizes they can simulate. To address these limitations, researchers have developed enhanced dynamics sampling techniques. For example, in the GLUT1 study by Park *et al.* [154], glucose binding and release were "forced" using a harmonic potential applied between the sugar molecule and the binding pocket, improving the efficiency of molecular dynamics simulations. However, classical and enhanced molecular dynamics are still restricted to small systems, which limits their ability to capture the broader context of ligand-receptor interactions at the BBB. These interactions are influenced by factors such as blood flow velocity, the presence of other proteins, ligands, and the glycocalyx environment. To overcome these challenges, coarse-graining methods have been introduced, allowing for the simulation of larger systems while maintaining essential molecular details, thus providing a more comprehensive view of complex biological processes. Coarse-graining refers to a series of methods that simplify simulations by reducing the number of particles being modelled. A good example of the application of coarse-grain methods is provided by Tial *et al.* [142], who, by using a well-established coarse-grained membrane surface path, were able to perform

a number of molecular dynamics simulations to capture the effect of avidity of BBB-targeted multivalent systems on membrane topological changes and nanoparticle aggregation dynamics.

As highlighted in this section, computational methods are now essential for studying receptor-ligand interactions. These methods complement experimental techniques by providing high-throughput insights into molecular dynamics, binding affinities, and structural predictions, which can speed up drug discovery and improve our understanding of complex biological systems. In the context of BBB crossing, there remains a gap in implementation, but we are optimistic that this gap will be filled soon as these technologies continue to advance and integrate more seamlessly into research and development processes.

5. Beyond the BBB: Reaching the target

At the structural level, the brain is organised in a highly complex multicellular network structurally supported by a dense matrix of proteins and polysaccharides, known as the ECM, whose spaces are filled with the ISF. The ISF facilitates the transport of molecules (for energy supply or communication) within the intercellular spaces and collaborates in clearing brain waste products. Once nanoparticles (or other brain therapeutics) successfully traverse the BBB, their journey within the brain involves navigating through the ISF while overcoming the physical barriers posed by the ECM until reaching their target. The process by which this transport occurs has not yet been fully elucidated and continues to be a matter of active debate.

In peripheral tissues, the movement of ISF is driven by a steady flow of plasma ultrafiltrate through fenestrated capillaries, with excess fluid and metabolic waste being drained away by lymphatic vessels. In the brain, given the lack of lymphatic vessels, ISF transport through the brain's extracellular space was traditionally described as relying on diffusion. This diffusive movement was driven by a slight hydrostatic pressure created by the secretion of fluid through the BBB that would drain out towards the CSF [158,159]. In accordance, molecule diffusion in the brain parenchyma has been demonstrated to be governed by three parameters: porosity (volume fraction) of the extracellular space that indicates the available space for diffusion; tortuosity, which quantifies the hindrance a molecule faces due to the brain's intricate structure; and, effective diffusivity that refers to the diffusion rate of a molecule within the brain tissue ([160] for a comprehensive review).

About a decade ago, the concept of the glymphatic system (GS) emerged, sparking ongoing discussions about the brain's fluid dynamics [158,161–164]. The GS was initially described as a clearance pathway in the CNS that helps remove brain waste products [165–167]. This system is driven by the rhythmic pulsations of cerebral arterial blood flow and facilitated by AQP-4 channels located at the endfeet of perivascular astrocytes. In this process, CSF flows from periarterial spaces into the brain's interstitial space, where it mixes with ISF. The mixed fluid is then propelled out of the brain through perivenous spaces, following a pressure gradient, thereby aiding in the clearance of ISF. Additional research on live mice (two-photon imaging) showed that GS activity follows endogenous circadian rhythms, with its function significantly enhanced during the sleep phase, allowing, for example, an increased rate of β -amyloid clearance during sleep [168].

So far, there is no consensus about solute transport in brain parenchyma. It most probably occurs through both diffusion and advection. The relative contributions of diffusion and advection may vary depending on spatial location and brain state. Future interdisciplinary studies focusing on the permeability of the extracellular space, solute concentration gradients, and the presence of pericapillary spaces, using techniques like MRI and super-resolution imaging, could provide further insights.

6. Better brain therapies: The future of computational and experimental Integration

Effective brain drug delivery remains a significant clinical challenge in treating CNS diseases, mainly due to the presence of the BBB. While our understanding of the BBB's complex and dynamic functions has improved, traditional drug delivery methods continue to face difficulties in safely and effectively penetrating this barrier. Despite the challenge, innovative strategies are emerging, notably towards enhancing the functionality of BBB “Trojan horses”. These strategies include the development of multivalent drug delivery systems, which may increase the specificity of BBB targeting, enhance the efficiency of BBB transcytosis, and potentially improve treatment efficacy. The super-selectivity offered by these multivalent systems shows promise in reducing off-target effects and enhancing therapeutic outcomes. Furthermore, there is increasing interest in integrating mathematical and computational modelling to advance these strategies. Such modelling enables the simulation of delivery systems interactions with the BBB and the optimisation of their design prior to experimental testing. Combining empirical findings with experimental validation will be crucial for developing more effective and clinically relevant brain drug delivery systems, ultimately leading to improved treatments for neurological diseases.

7. Funding sources

This work was supported by the European Union's Horizon Europe research and innovation program (Marie Skłodowska-Curie grant agreement No. 101066836), ‘La Caixa’ Foundation (ID 100010434; LCF/BQ/DI22/11940010), ERC Consolidator grant H2020-ERC-2018-CoG (769798 ChesSTag), Plan de Recuperación Nacional Biotech for Health Project (ADNano), Alzheimer's Association New to the Field award, Activitat científica dels grups de recerca de Catalunya (SGR-Cat 2021), and Spanish Research Agency Proyectos I + D + I PID2020-119914RB-I00.

Data availability

No data was used for the research described in the article.

References

- [1] K. Morris, M. Nami, J.F. Bolanos, M.A. Lobo, M. Sadri-Naini, J. Fiallos, G. E. Sanchez, T. Bustos, N. Chintam, M. Amaya, S.E. Strand, A. Mayuku-Dore, I. Sakibova, G.M.N. Biso, A. Defilippis, D. Bravo, N. Tarhan, C. Claussen, A. Mercado, S. Braun, L. Yuge, S. Okabe, F. Taghizadeh-Hesary, K. Kotliar, C. Sadowsky, P.S. Chandra, M. Tripathi, V. Katsaros, B. Mehling, M. Noroozian, K. Abbasioun, A. Amirjamshidi, G.A. Hossein-Zadeh, F. Naraghi, M. Barzegar, A. A. Asadi-Pooya, S. Sahab-Negah, S. Sadeghian, M. Fahnestock, N. Dilbaz, N. Hussain, Z. Mari, R.W. Thatcher, D. Sipple, K. Sidhu, D. Chopra, F. Costa, G. Spena, T. Berger, D. Zelinsky, C.J. Wheeler, J.W. Ashford, R. Schulte, M. A. Nezami, H. Kloor, A. Filler, D.S. Eliashiv, Di. Sinha, A.A.F. Desalles, V. Sadanand, S. Suchkov, K. Green, B. Metin, R. Hariri, J. Cormier, V. Yamamoto, B. Kateb, Neuroscience20 (BRAIN20, SPINE20, and MENTAL20) health Initiative: a global consortium addressing the human and economic burden of brain, spine, and mental disorders through neurotech innovations and policies, J. Alzheimers Dis. 83 (2021) 1563–1601, <https://doi.org/10.3233/JAD-215190>.
- [2] G.E. E., Die aussere und innere Sekretion des gesunden und kranken Organismus im Lichte der “vitalen Farbung,” Beitr. Klin. Chir. 64 (1909) 192–265. <https://cir.nii.ac.jp/crid/1571980075031708544> (accessed January 11, 2025).
- [3] L. M., Zur Lehre der Cerebrospinalflussigkeit, Z. Klin. Med. 40 (1909) 480–494. <https://cir.nii.ac.jp/crid/1572824499961844096> (accessed January 11, 2025).
- [4] T.S. Reese, M.J. Karnovsky, Fine structural localization of a blood-brain barrier to exogenous peroxidase, J. Cell Biol. 34 (1967) 207–217, <https://doi.org/10.1083/jcb.34.1.207>.
- [5] N.J. Abbott, A.A.K. Patabendige, D.E.M. Dolman, S.R. Yusof, D.J. Begley, Structure and function of the blood–brain barrier, Neurobiol. Dis. 37 (2010) 13–25, <https://doi.org/10.1016/j.nbd.2009.07.030>.
- [6] B.T. Hawkins, T.P. Davis, The blood-brain barrier/neurovascular unit in health and disease, Pharmacol. Rev. 57 (2005) 173–185, <https://doi.org/10.1124/PR.57.2.4>.
- [7] P. Solár, A. Zamani, L. Kubícková, P. Dubový, M. Joukal, Choroid plexus and the blood–cerebrospinal fluid barrier in disease, Fluids and Barriers of the CNS 2020 17:1 17 (2020) 1–29. doi: 10.1186/S12987-020-00196-2.
- [8] H. Tuman, A. Huss, F. Bachhuber, The cerebrospinal fluid and barriers – anatomic and physiologic considerations, in: Handb Clin Neurol, Elsevier B.V., 2017: pp. 3–20. doi: 10.1016/B978-0-12-804279-3.00002-2.
- [9] W.M. Pardridge, Blood-brain barrier endogenous transporters as therapeutic targets: a new model for small molecule CNS drug discovery, Expert Opin. Ther. Targets 19 (2015) 1059–1072, <https://doi.org/10.1517/14728222.2015.1042364>.
- [10] M.D. Sweeney, Z. Zhao, A. Montagne, A.R. Nelson, B.V. Zlokovic, From physiology to disease and back, Physiol. Rev. 99 (2019) 21–78, <https://doi.org/10.1152/physrev.00050.2017-The>.
- [11] A. Montagne, Z. Zhao, B.V. Zlokovic, Alzheimer's disease: a matter of blood–brain barrier dysfunction? J. Exp. Med. 214 (2017) 3151–3169, <https://doi.org/10.1084/JEM.20171406>.
- [12] Z. Zhao, A.R. Nelson, C. Betsholtz, B.V. Zlokovic, Establishment and dysfunction of the blood-brain barrier, Cell 163 (2015) 1064–1078, <https://doi.org/10.1016/j.cell.2015.10.067>.
- [13] K. Kisler, A.R. Nelson, A. Montagne, B.V. Zlokovic, Cerebral blood flow regulation and neurovascular dysfunction in Alzheimer disease, Nat. Rev. Neurosci. 18 (2017) 419–434, <https://doi.org/10.1038/NRN.2017.48>.
- [14] N.R. Saunders, K.M. Dziegielewska, K. Møllgård, M.D. Habgood, Physiology and molecular biology of barrier mechanisms in the fetal and neonatal brain, J. Physiol. 596 (2018) 5723–5756, <https://doi.org/10.1113/JP275376>.
- [15] A. Kabelev, V. Lobaskin, Structure and elasticity of bush and brush-like models of the endothelial glycocalyx, Sci. Rep. 2017 8:1 8 (2018) 1–13. doi: 10.1038/s41598-017-18577-3.
- [16] S.C. Purcell, K. Godula, Synthetic glycocalyx: addressing the structural and functional complexity of the glycocalyx, J. R. Soc. Interface Focus 9 (2019), <https://doi.org/10.1098/RSFS.2018.0080>.
- [17] H.W. Song, K.L. Foreman, B.D. Gastfriend, J.S. Kuo, S.P. Palecek, E. V. Shusta, Transcriptomic comparison of human and mouse brain microvessels, Sci. Rep. 2020 10:1 10 (2020) 1–14. doi: 10.1038/s41598-020-69096-7.
- [18] S. Reitsma, D.W. Slaaf, H. Vink, M.A.M.J. Van Zandvoort, M.G.A. Oude Egbrink, The endothelial glycocalyx: composition, functions, and visualization, Pflügers Arch 454 (2007) 345–359. doi: 10.1007/s00424-007-0212-8.
- [19] C. Rüegg, A. Mariotti, Vascular integrins: pleiotropic adhesion and signaling molecules in vascular homeostasis and angiogenesis, Cell. Mol. Life Sci. 60 (2003) 1135, <https://doi.org/10.1007/S00018-003-2297-3>.
- [20] H. Kadry, B. Noorani, L. Cucullo, A blood-brain barrier overview on structure, function, impairment, and biomarkers of integrity, Fluids Barriers CNS 17 (2020), <https://doi.org/10.1186/s12987-020-00230-3>.
- [21] F. Sanchez-Cano, L.C. Hernández-Kelly, A. Ortega, The blood–brain barrier: much more than a selective access to the brain, Neurotox. Res. 39 (2021) 2154–2174, <https://doi.org/10.1007/S12640-021-00431-0>.
- [22] N.J. Abbott, Dynamics of CNS barriers: Evolution, differentiation, and modulation, Cell. Mol. Neurobiol. 25 (2005) 5–23, <https://doi.org/10.1007/s10571-004-1374-y>.
- [23] B. Srinivasan, A.R. Kolli, M.B. Esch, H.E. Abaci, M.L. Shuler, J.J. Hickman, TEER measurement techniques for in vitro barrier model systems, (n.d.). doi: 10.1177/2211068214561025.
- [24] W.H. Oldendorf, M.E. Cornford, W.J. Brown, The large apparent work capability of the blood-brain barrier: a study of the mitochondrial content of capillary endothelial cells in brain and other tissues of the rat, Ann. Neurol. 1 (1977) 409–417, <https://doi.org/10.1002/ANA.410010502>.
- [25] G. Bazzoni, E. Dejana, Endothelial cell-to-cell junctions: Molecular organization and role in vascular homeostasis, Physiol. Rev. 84 (2004) 869–901, <https://doi.org/10.1152/PHYSREV.00035.2003>.
- [26] M. Sans, S. Kawachi, A. Soriano, A. Palacín, Z. Morise, D.N. Granger, J.M. Piqué, M.B. Grisham, J. Panés, Brain endothelial adhesion molecule expression in experimental colitis, Microcirculation 8 (2001) 105–114, <https://doi.org/10.1111/J.1549-8719.2001.TB00161.X>.
- [27] K. Kisler, A.R. Nelson, S. V. Rege, A. Ramanathan, Y. Wang, A. Ahuja, D. Lazic, P. S. Tsai, Z. Zhao, Y. Zhou, D.A. Boas, S. Sakadžić, B. V. Zlokovic, Pericyte degeneration leads to neurovascular uncoupling and limits oxygen supply to brain, Nature Neuroscience 2017 20:3 20 (2017) 406–416. doi: 10.1038/nn.4489.
- [28] I. Galea, The blood–brain barrier in systemic infection and inflammation, Cellular & Molecular Immunology 2021 18:11 18 (2021) 2489–2501. doi: 10.1038/s41423-021-00757-x.
- [29] S. Hori, S. Ohtsuki, K.I. Hosoya, E. Nakashima, T. Terasaki, A pericyte-derived angiopoietin-1 multimeric complex induces occludin gene expression in brain capillary endothelial cells through Tie-2 activation in vitro, J. Neurochem. 89 (2004) 503–513, <https://doi.org/10.1111/J.1471-4159.2004.02343.X>.
- [30] A.M. Nikolakopoulou, A. Montagne, K. Kisler, Z. Dai, Y. Wang, M.T. Huuskonen, A.P. Sagare, D. Lazic, M.D. Sweeney, P. Kong, M. Wang, N.C. Owens, E.J. Lawson, X. Xie, Z. Zhao, B.V. Zlokovic, Pericyte loss leads to circulatory failure and pleiotrophin depletion causing neuron loss, Nat. Neurosci. (2019) 1089–1098, <https://doi.org/10.1038/s41593-019-0434-z>.
- [31] M. Hellström, H. Gerhardt, M. Kalén, X. Li, U. Eriksson, H. Wolburg, C. Betsholtz, Lack of pericytes leads to endothelial hyperplasia and abnormal vascular morphogenesis, J. Cell Biol. 153 (2001) 543–554, <https://doi.org/10.1083/JCB.153.3.543>.
- [32] L. Xu, A. Nirwane, Y. Yao, Basement membrane and blood–brain barrier, Stroke Vasc. Neurol. 4 (2019) 78–82, <https://doi.org/10.1136/SVN-2018-000198>.

- [33] M.D. Sweeney, S. Ayyadurai, B.V. Zlokovic, Pericytes of the neurovascular unit: key functions and signaling pathways, *Nat. Neurosci.* 19 (2016) 771–783, <https://doi.org/10.1038/NN.4288>.
- [34] R.D. Bell, E.A. Winkler, A.P. Sagare, I. Singh, B. LaRue, R. Deane, B.V. Zlokovic, Pericytes control key neurovascular functions and neuronal phenotype in the adult brain and during brain aging, *Neuron* 68 (2010) 409–427, <https://doi.org/10.1016/j.neuron.2010.09.043>.
- [35] A. Bhattacharya, D.K. Kaushik, B.M. Lozinski, V.W. Yong, Beyond barrier functions: Roles of pericytes in homeostasis and regulation of neuroinflammation, *J. Neurosci. Res.* 98 (2020) 2390–2405, <https://doi.org/10.1002/JNR.24715>.
- [36] S. Noell, K. Wolburg-Buchholz, A.F. Mack, A.M. Beedle, J.S. Satz, K.P. Campbell, H. Wolburg, P. Fallier-Becker, Evidence for a role of dystroglycan regulating the membrane architecture of astroglial endfeet, *Eur. J. Neurosci.* 33 (2011) 2179, <https://doi.org/10.1111/J.1460-9568.2011.07688.X>.
- [37] N.J. Abbott, L. Rönnbäck, E. Hansson, Astrocyte-endothelial interactions at the blood-brain barrier, *Nat. Rev. Neurosci.* 7 (2006) 41–53, <https://doi.org/10.1038/nrn1824>.
- [38] R.C. Janzer, M.C. Raff, Astrocytes induce blood-brain barrier properties in endothelial cells, *Nature* 1987 325:6101 325 (1987) 253–257. doi: 10.1038/325253a0.
- [39] A. Hoshi, T. Yamamoto, K. Shimizu, Y. Sugiura, Y. Ugawa, Chemical preconditioning-induced reactive astrocytosis contributes to the reduction of post-ischemic edema through aquaporin-4 downregulation, *Exp. Neurol.* 227 (2011) 89–95, <https://doi.org/10.1016/j.expneurol.2010.09.016>.
- [40] S.M. Theparambil, G. Begum, C.R. Rose, pH regulating mechanisms of astrocytes: a critical component in physiology and disease of the brain, *Cell Calcium* 120 (2024) 102882, <https://doi.org/10.1016/j.ceca.2024.102882>.
- [41] G.R. Frost, Y.M. Li, The role of astrocytes in amyloid production and Alzheimer's disease, *Open Biol.* 7 (2017) 170228, <https://doi.org/10.1098/RSOB.170228>.
- [42] M. Asgari, D. De Zélicourt, V. Kurtcuoglu, How astrocyte networks may contribute to cerebral metabolite clearance, *Sci. Rep.* 5 (2015), <https://doi.org/10.1038/SREP15024>.
- [43] L. Xu, A. Nirwane, Y. Yao, Basement membrane and blood-brain barrier, *Stroke Vasc. Neurol.* 4 (2018) 78, <https://doi.org/10.1136/SVN-2018-000198>.
- [44] C. Wu, F. Ivars, P. Anderson, R. Hallmann, D. Vestweber, P. Nilsson, H. Robenek, K. Tryggvason, J. Song, E. Korpos, K. Loser, S. Beissert, E. Georges-Labouesse, L. M. Sorokin, Endothelial basement membrane laminin alpha5 selectively inhibits T lymphocyte extravasation into the brain, *Nat. Med.* 15 (2009) 519–527, <https://doi.org/10.1038/NM.1957>.
- [45] M. Sixt, B. Engelhardt, F. Pausch, R. Hallmann, O. Wendler, L.M. Sorokin, Endothelial cell laminin isoforms, laminins 8 and 10, play decisive roles in T cell recruitment across the blood-brain barrier in experimental autoimmune encephalomyelitis, *J. Cell Biol.* 153 (2001) 933, <https://doi.org/10.1083/JCB.153.5.933>.
- [46] H.K. Alajangi, M. Kaur, A. Sharma, S. Rana, S. Thakur, M. Chatterjee, N. Singla, P. K. Jaiswal, G. Singh, R.P. Barnwal, Blood-brain barrier: emerging trends on transport models and new-age strategies for therapeutics intervention against neurological disorders, *Molecular Brain* 2022 15:1 15 (2022) 1–28. doi: 10.1186/S13041-022-00937-4.
- [47] Z.L. Chen, W.M. Yu, S. Strickland, Peripheral regeneration, *Annu. Rev. Neurosci.* 30 (2007) 209–233, <https://doi.org/10.1146/ANNUREV.NEURO.30.051606.094337>.
- [48] Y. Yao, Z.L. Chen, E.H. Norris, S. Strickland, Astrocytic laminin regulates pericyte differentiation and maintains blood brain barrier integrity, *Nat. Commun.* 2014 5: 1 5 (2014) 1–12. doi: 10.1038/ncomms4413.
- [49] A.-C. Luissint, C. Artus, F. Glacial, K. Ganeshamoorthy, P.-O. Couraud, Tight junctions at the blood brain barrier: physiological architecture and disease-associated dysregulation, *Fluids Barriers CNS* 9 (2012) 23, <https://doi.org/10.1186/2045-8118-9-23>.
- [50] K. Krishna, C. Redies, Expression of cadherin superfamily genes in brain vascular development, *J. Cereb. Blood Flow Metab.* 29 (2009) 224–229, <https://doi.org/10.1038/jcbfm.2008.123>.
- [51] S. Tietz, B. Engelhardt, Brain barriers: Crosstalk between complex tight junctions and adherens junctions, *J. Cell Biol.* 209 (2015) 493–506, <https://doi.org/10.1083/jcb.201412147>.
- [52] B.V. Zlokovic, The blood-brain barrier in health and chronic neurodegenerative disorders, *Neuron* 57 (2008) 178–201, <https://doi.org/10.1016/j.neuron.2008.01.003>.
- [53] A.M. Butt, H.C. Jones, N.J. Abbott, Electrical resistance across the blood-brain barrier in anaesthetized rats: a developmental study, *J. Physiol.* 429 (1990) 47–62, <https://doi.org/10.1113/jphysiol.1990.sp018243>.
- [54] K. Shin, V.C. Fogg, B. Margolis, Tight junctions and cell polarity, *Annu. Rev. Cell Dev. Biol.* 22 (2006) 207–235, <https://doi.org/10.1146/annurev.cellbio.22.010305.104219>.
- [55] S. Dithmer, I.E. Blasig, P.A. Fraser, Z. Qin, R.F. Haseloff, The basic requirement of tight junction proteins in blood-brain barrier function and their role in pathologies, *Int. J. Mol. Sci.* 25 (2024) 5601, <https://doi.org/10.3390/ijms25115601>.
- [56] R. Daneman, L. Zhou, D. Agalliu, J.D. Cahoy, A. Kaushal, B.A. Barres, The mouse blood-brain barrier transcriptome: a new resource for understanding the development and function of brain endothelial cells, *PLoS One* 5 (2010) e13741, <https://doi.org/10.1371/journal.pone.0013741>.
- [57] T. Nitta, M. Hata, S. Gotoh, Y. Seo, H. Sasaki, N. Hashimoto, M. Furuse, S. Tsukita, Size-selective loosening of the blood-brain barrier in claudin-5-deficient mice, *J. Cell Biol.* 161 (2003) 653–660, <https://doi.org/10.1083/jcb.200302070>.
- [58] P. Berndt, L. Winkler, J. Cording, O. Breitkreuz-Korff, A. Rex, S. Dithmer, V. Rausch, R. Blasig, M. Richter, A. Sporbert, H. Wolburg, I.E. Blasig, R. F. Haseloff, Tight junction proteins at the blood-brain barrier: far more than claudin-5, *Cell. Mol. Life Sci.* 76 (2019) 1987–2002, <https://doi.org/10.1007/s00018-019-03030-7>.
- [59] M. Lal-Nag, P.J. Morin, The claudins, *Genome Biol.* 10 (2009) 235, <https://doi.org/10.1186/gb-2009-10-8-235>.
- [60] M. Furuse, T. Hirase, M. Itoh, A. Nagafuchi, S. Yonemura, S. Tsukita, S. Tsukita, Occludin: a novel integral membrane protein localizing at tight junctions, *J. Cell Biol.* 123 (1993) 1777–1788, <https://doi.org/10.1083/jcb.123.6.1777>.
- [61] V. Wong, Phosphorylation of occludin correlates with occludin localization and function at the tight junction, *Am. J. Phys. Cell Phys.* 273 (1997) C1859–C1867, <https://doi.org/10.1152/ajpcell.1997.273.6.C1859>.
- [62] I.E. Blasig, C. Bellmann, J. Cording, G. del Vecchio, D. Zwanziger, O. Huber, R. F. Haseloff, Occludin protein family: oxidative stress and reducing conditions, *Antioxid. Redox Signal.* 15 (2011) 1195–1219, <https://doi.org/10.1089/ars.2010.3542>.
- [63] N.S. Harhaj, E.A. Felinski, E.B. Wolpert, J.M. Sundstrom, T.W. Gardner, D. A. Antonetti, VEGF activation of protein kinase C stimulates occludin phosphorylation and contributes to endothelial permeability, *Investigative Ophthalmology & Visual Science* 47 (2006) 5106, <https://doi.org/10.1167/iovs.06-0322>.
- [64] M. Saitou, M. Furuse, H. Sasaki, J.-D. Schulzke, M. Fromm, H. Takano, T. Noda, S. Tsukita, Complex phenotype of mice lacking occludin, a component of tight junction strands, *Mol. Biol. Cell* 11 (2000) 4131–4142, <https://doi.org/10.1091/mbc.11.12.4131>.
- [65] M. Saitou, K. Fujimoto, Y. Doi, M. Itoh, T. Fujimoto, M. Furuse, H. Takano, T. Noda, S. Tsukita, Occludin-deficient embryonic stem cells can differentiate into polarized epithelial cells bearing tight junctions, *J. Cell Biol.* 141 (1998) 397–408, <https://doi.org/10.1083/jcb.141.2.397>.
- [66] R.M. Bendriem, S. Singh, A.A. Aleem, D.A. Antonetti, M.E. Ross, Tight junction protein occludin regulates progenitor Self-Renewal and survival in developing cortex, *Life* 8 (2019), <https://doi.org/10.7554/eLife.49376>.
- [67] S. Tsukita, M. Furuse, M. Itoh, Multifunctional strands in tight junctions, *Nat. Rev. Mol. Cell Biol.* 2 (2001) 285–293, <https://doi.org/10.1038/35067088>.
- [68] S. Garrido-Urbani, P.F. Bradfield, B.A. Imhof, Tight junction dynamics: the role of junctional adhesion molecules (JAMs), *Cell Tissue Res.* 355 (2014) 701–715, <https://doi.org/10.1007/s00441-014-1820-1>.
- [69] E.E. Schneeberger, R.D. Lynch, The tight junction: a multifunctional complex, *Am. J. Phys. Cell Phys.* 286 (2004) C1213–C1228, <https://doi.org/10.1152/ajpcell.00558.2003>.
- [70] L.S. Rodgers, M.T. Beam, J.M. Anderson, A.S. Fanning, Epithelial barrier assembly requires coordinated activity of multiple domains of the tight junction protein ZO-1, *J. Cell Sci.* (2013), <https://doi.org/10.1242/jcs.113399>.
- [71] H.-C. Bauer, I.A. Krizbai, H. Bauer, A. Traweger, “You shall not pass”—tight junctions of the blood brain barrier, *Front. Neurosci.* 8 (2014), <https://doi.org/10.3389/fnins.2014.00392>.
- [72] A.H. Schinkel, J.W. Jonker, Mammalian drug efflux transporters of the ATP binding cassette (ABC) family: an overview, *Adv. Drug Deliv. Rev.* 55 (2003) 3–29, [https://doi.org/10.1016/S0169-409X\(02\)00169-2](https://doi.org/10.1016/S0169-409X(02)00169-2).
- [73] M. Demeule, A. Régina, J. Jodoin, A. Laplante, C. Dagenais, F. Berthelot, A. Moghrabi, R. Béliveau, Drug transport to the brain: key roles for the efflux pump P-glycoprotein in the blood-brain barrier, *Vasc. Pharmacol.* 38 (2002) 339–348, [https://doi.org/10.1016/S1373-1891\(02\)00201-X](https://doi.org/10.1016/S1373-1891(02)00201-X).
- [74] P.L. Golden, G.M. Pollack, Blood-brain barrier efflux transporter, *J. Pharm. Sci.* 92 (2003) 1739–1753, <https://doi.org/10.1002/jps.10424>.
- [75] D. Begley, ABC transporters and the blood-brain barrier, *Curr. Pharm. Des.* 10 (2004) 1295–1312, <https://doi.org/10.2174/1381612043384844>.
- [76] F.J. Sharom, The P-glycoprotein multidrug transporter, *Essays Biochem.* 50 (2011) 161–178, <https://doi.org/10.1042/bse0500161>.
- [77] Y. Kim, J. Chen, Molecular structure of human P-glycoprotein in the ATP-bound, outward-facing conformation, *Science* 359 (2018) 915–919, <https://doi.org/10.1126/science.aar7389>.
- [78] G. Tomblin, L.A. Bartholomew, I.L. Urbatsch, A.E. Senior, Combined mutation of catalytic glutamate residues in the two nucleotide binding domains of P-glycoprotein generates a conformation that binds ATP and ADP tightly, *J. Biol. Chem.* 279 (2004) 31212–31220, <https://doi.org/10.1074/jbc.M404689200>.
- [79] S.V. Ambudkar, C. Kimchi-Sarfaty, Z.E. Sauna, M.M. Gottesman, P-glycoprotein: from genomics to mechanism, *Oncogene* 22 (2003) 7468–7485, <https://doi.org/10.1038/sj.onc.1206948>.
- [80] W. Löscher, H. Potschka, Blood-brain barrier active efflux transporters: ATP-binding cassette gene family, *NeuroRx* 2 (2005) 86–98, <https://doi.org/10.1602/neuroRx.2.1.86>.
- [81] K. Yano, T. Tomono, T. Ogihara, Advances in studies of P-glycoprotein and its expression regulators, *Biol. Pharm. Bull.* 41 (2018) 11–19, <https://doi.org/10.1248/bpb.b17-00725>.
- [82] M. Elmeliyeg, M. Vourvahis, C. Guo, D.D. Wang, Effect of P-glycoprotein (P-gp) inducers on exposure of P-gp substrates: review of clinical drug-drug interaction studies, *Clin. Pharmacokinet.* 59 (2020) 699–714, <https://doi.org/10.1007/s40262-020-00867-1>.
- [83] S. Cisternino, C. Mercier, F. Bourasset, F. Roux, J.-M. Scherrmann, Expression, up-regulation, and transport activity of the multidrug-resistance protein Abcg2 at the mouse blood-brain barrier, *Cancer Res.* 64 (2004) 3296–3301, <https://doi.org/10.1158/0008-5472.CAN-03-2033>.
- [84] T. Eisenblätter, S. Hüwel, H.-J. Galla, Characterisation of the brain multidrug resistance protein (BMDP/ABCG2/BCRP) expressed at the blood-brain barrier,

- Brain Res. 971 (2003) 221–231, [https://doi.org/10.1016/S0006-8993\(03\)02401-6](https://doi.org/10.1016/S0006-8993(03)02401-6).
- [85] H.C. Cooray, C.G. Blackmore, L. Maskell, M.A. Barrand, Localisation of breast cancer resistance protein in microvessel endothelium of human brain, *Neuroreport* 13 (2002) 2059–2063, <https://doi.org/10.1097/00001756-200211150-00014>.
- [86] A.T. Nies, F. Klein, Multidrug resistance proteins of the ABCG subfamily, in: *Drug Transporters*, Wiley, 2022: pp. 213–233. doi: 10.1002/9781119739883.ch11.
- [87] R.G. Deeley, C. Westlake, S.P.C. Cole, Transmembrane transport of endo- and xenobiotics by mammalian ATP-binding cassette multidrug resistance proteins, *Physiol. Rev.* 86 (2006) 849–899, <https://doi.org/10.1152/physrev.00035.2005>.
- [88] Y. Zhang, H. Han, W.F. Elmquist, D.W. Miller, Expression of various multidrug resistance-associated protein (MRP) homologues in brain microvessel endothelial cells, *Brain Res.* 876 (2000) 148–153, [https://doi.org/10.1016/S0006-8993\(00\)02628-7](https://doi.org/10.1016/S0006-8993(00)02628-7).
- [89] A.T. Nies, G. Jedlitschky, J. König, C. Herold-Mende, H.H. Steiner, H.-P. Schmitt, D. Keppler, Expression and immunolocalization of the multidrug resistance proteins, MRP1–MRP6 (ABCC1–ABCC6), in human brain, *Neuroscience* 129 (2004) 349–360, <https://doi.org/10.1016/j.neuroscience.2004.07.051>.
- [90] U.H. Langen, S. Ayloo, C. Gu, Annual Review of Cell and Developmental Biology Development and Cell Biology of the Blood-Brain Barrier (2019), <https://doi.org/10.1146/annurev-cellbio-100617>.
- [91] A. César-Razquin, B. Snijder, T. Frappier-Brinton, R. Isserlin, G. Gyimesi, X. Bai, R.A. Reithmeier, D. Hepworth, M.A. Hediger, A.M. Edwards, G. Superti-Furga, A call for systematic research on solute carriers, *Cell* 162 (2015) 478–487, <https://doi.org/10.1016/j.cell.2015.07.022>.
- [92] C. Tiruppathi, A. Finnegan, A.B. Malik, Isolation and characterization of a cell surface albumin-binding protein from vascular endothelial cells, *Proc. Natl. Acad. Sci. U. S. A.* 93 (1996) 250–254, <https://doi.org/10.1073/PNAS.93.1.250>.
- [93] U. Bickel, T. Yoshikawa, W.M. Pardridge, Delivery of peptides and proteins through the blood-brain barrier, *Adv. Drug Deliv. Rev.* 46 (2001) 247–279, [https://doi.org/10.1016/S0169-409X\(00\)00139-3](https://doi.org/10.1016/S0169-409X(00)00139-3).
- [94] X. Zhu, K. Jin, Y. Huang, Z. Pang, Brain drug delivery by adsorption-mediated transcytosis, *Brain Targeted Drug Delivery Systems: A Focus on Nanotechnology and Nanoparticulates* (2019) 159–183, <https://doi.org/10.1016/B978-0-12-814001-7.00007-X>.
- [95] G. Hong, O. Chappey, E. Niel, J.M. Scherrmann, Enhanced cellular uptake and transport of polyclonal immunoglobulin G and fab after their cationization, *J. Drug Target.* 8 (2000) 67–77, <https://doi.org/10.3109/10611860008996853>.
- [96] A.S. Haqqani, K. Bélanger, D.B. Stanimirovic, Receptor-mediated transcytosis for brain delivery of therapeutics: receptor classes and criteria, *Front. Drug Delivery* 4 (2024), <https://doi.org/10.3389/FDDEV.2024.1360302>.
- [97] W.M. Pardridge, J. Eisenberg, J. Yang, Human blood–brain barrier insulin receptor, *J. Neurochem.* 44 (1985) 1771–1778, <https://doi.org/10.1111/J.1471-4159.1985.TB07167.X>.
- [98] H. Werner, D. Weinstein, I. Bentov, Similarities and differences between insulin and IGF-I: structures, receptors, and signalling pathways, *Arch. Physiol. Biochem.* 114 (2008) 17–22, <https://doi.org/10.1080/13813450801900694>.
- [99] J.J. Kim, D. Accili, Signalling through IGF-I and insulin receptors: where is the specificity? *Growth Hormone and IGF Research* 12 (2002) 84–90, <https://doi.org/10.1054/ghir.2002.0265>.
- [100] A. Dautry Varsat, A. Ciechanover, H.F. Lodish, pH and the recycling of transferrin during receptor-mediated endocytosis, *Proc. Natl. Acad. Sci. U. S. A.* 80 (1983) 2258–2262, <https://doi.org/10.1073/PNAS.80.8.2258>.
- [101] K.A. Duck James R Connor, Iron uptake and transport across physiological barriers, (n.d.). doi: 10.1007/s10534-016-9952-2.
- [102] J.J. Hill, A.S. Haqqani, D.B. Stanimirovic, Proteome of the luminal surface of the blood–brain barrier, *Proteomes* 9 (2021), <https://doi.org/10.3390/PROTEOMES9040045>.
- [103] Y. Li, J. Cam, G. Bu, Low-density lipoprotein receptor family: endocytosis and signal transduction, *Mol. Neurobiol.* 23 (2001) 53–67, <https://doi.org/10.1385/MN:23:1:53>.
- [104] E. Mantuano, P. Azmoon, M.A. Banki, C.B. Gunner, S.L. Gonias, The LRP1/CD91 ligands, tissue-type plasminogen activator, α 2-macroglobulin, and soluble cellular prion protein have distinct co-receptor requirements for activation of cell-signaling, *Sci. Rep.* 12 (12344) 17594. doi: 10.1038/s41598-022-22498-1.
- [105] S.L. Gonias, W.M. Campana, LDL receptor-related protein-1: a regulator of inflammation in atherosclerosis, cancer, and injury to the nervous system, *Am. J. Pathol.* 184 (2014) 18–27, <https://doi.org/10.1016/j.ajpath.2013.08.029>.
- [106] R.A. Fuentealba, Q. Liu, T. Kanekiyo, J. Zhang, G. Bu, Low density lipoprotein receptor-related protein 1 promotes anti-apoptotic signaling in neurons by activating Akt survival pathway, *J. Biol. Chem.* 284 (2009) 34045–34053, <https://doi.org/10.1074/JBC.M109.021030>.
- [107] Y. Li, W. Lu, G. Bu, Essential role of the low density lipoprotein receptor-related protein in vascular smooth muscle cell migration, *FEBS Lett.* 555 (2003) 346–350, [https://doi.org/10.1016/S0014-5793\(03\)01272-9](https://doi.org/10.1016/S0014-5793(03)01272-9).
- [108] F.M.G. Cornelissen, G. Markert, G. Deutsch, M. Antonara, N. Faaij, I. Bartelink, D. Noske, W.P. Vandertop, A. Bender, B.A. Westerman, Explaining blood-brain barrier permeability of small molecules by integrated analysis of different transport mechanisms, *J. Med. Chem.* 66 (2023) 7253–7267, <https://doi.org/10.1021/ACS.JMEDCHEM.2C01824>.
- [109] A. Finch, P. Pillars, P-glycoprotein and its role in drug-drug interactions, *Aust. Prescr.* 37 (2014) 137–139, <https://doi.org/10.18773/AUSTPRESCR.2014.050>.
- [110] T. Kageyama, M. Nakamura, A. Matsuo, Y. Yamasaki, Y. Takakura, M. Hashida, Y. Kanai, M. Naito, T. Tsuruo, N. Minato, S. Shimohama, The 4F2hc/LAT1 complex transports L-DOPA across the blood-brain barrier, *Brain Res.* 879 (2000) 115–121, [https://doi.org/10.1016/S0006-8993\(00\)02758-X](https://doi.org/10.1016/S0006-8993(00)02758-X).
- [111] G.J. Goldenberg, H.-Y.-P. Lam, A. Begleiter, Active carrier-mediated transport of melphalan by two separate amino acid transport systems in LPC-1 plasmacytoma cells in vitro*, *J. B~or.Ocr~ CHEMI~TRY* 54 (1979) 105–1064, [https://doi.org/10.1016/S0021-9258\(17\)34167-4](https://doi.org/10.1016/S0021-9258(17)34167-4).
- [112] H. Uchino, Y. Kanai, D.K. Kim, M.F. Wempe, A. Chairoungdua, E. Morimoto, M. W. Anders, H. Endou, Transport of amino acid-related compounds mediated by L-type amino acid transporter 1 (LAT1): insights into the mechanisms of substrate recognition, *Mol. Pharmacol.* 61 (2002) 729–737, <https://doi.org/10.1124/MOL.61.4.729>.
- [113] M. Saeedi, M. Eslamifar, K. Khezri, S.M. Dizaj, Applications of nanotechnology in drug delivery to the central nervous system, *Biomed. Pharmacother.* 111 (2019) 666–675, <https://doi.org/10.1016/J.BIOPHA.2018.12.133>.
- [114] S. Sharma, S. Dang, Nanocarrier-based drug delivery to brain: interventions of surface modification, *Curr. Neuropharmacol.* 21 (2023) 517, <https://doi.org/10.2174/1570159X20666220706121412>.
- [115] F. Rehan, M. Zhang, J. Fang, K. Greish, Therapeutic applications of nanomedicine: recent developments and future perspectives, *Molecules* 29 (2024) 2073, <https://doi.org/10.3390/MOLECULES29092073>.
- [116] Chimeric peptides for neuropeptide delivery through the blood-brain barrier, (1987).
- [117] A. Cignarelli, V.A. Genchi, S. Perrini, A. Natalicchio, L. Laviola, F. Giorgino, Insulin and insulin receptors in adipose tissue development, *Int. J. Mol. Sci.* 20 (2019), <https://doi.org/10.3390/IJMS20030759>.
- [118] L.H. Dieu, D. Wu, C.G. Palivan, V. Balasubramanian, J. Huwyler, Polymersomes conjugated to 83-14 monoclonal antibodies: In vitro targeting of brain capillary endothelial cells, *Eur. J. Pharm. Biopharm.* 88 (2014) 316–324, <https://doi.org/10.1016/J.EJPB.2014.05.021>.
- [119] R.J. Boado, E.K.W. Hui, J. Zhiqiang Lu, W.M. Pardridge, Drug targeting of erythropoietin across the primate blood-brain barrier with an IgG molecular trojan horse, *J. Pharmacol. Exp. Therapeutics* 333 (2010) 961–969, <https://doi.org/10.1124/JPET.109.165092>.
- [120] H. Gao, S. Zhang, S. Cao, Z. Yang, Z. Pang, X. Jiang, Angiopep-2 and activatable cell-penetrating peptide dual-functionalized nanoparticles for systemic glioma-targeting delivery, *Mol. Pharm.* 11 (2014) 2755–2763, <https://doi.org/10.1021/MP500113P>.
- [121] K. Sakamoto, Generation of KS-487 as a novel LRP1-binding cyclic peptide with higher affinity, higher stability and BBB permeability, *Biochem. Biophys. Rep.* 32 (2022) 101367, <https://doi.org/10.1016/J.BBREP.2022.101367>.
- [122] K. Sakamoto, T. Shinohara, Y. Adachi, T. Asami, T. Ohtaki, A novel LRP1-binding peptide L57 that crosses the blood brain barrier, *Biochem. Biophys. Rep.* 12 (2017) 135, <https://doi.org/10.1016/J.BBREP.2017.07.003>.
- [123] T.J. Esparza, S. Su, C.M. Francescutti, E. Rodionova, J.H. Kim, D.L. Brody, Enhanced in vivo blood brain barrier transcytosis of macromolecular cargo using an engineered pH-sensitive mouse transferrin receptor binding nanobody, *Fluids Barriers CNS* 20 (2023), <https://doi.org/10.1186/s12987-023-00462-z>.
- [124] N. Bien-Ly, Y.J. Yu, D. Bumbaca, J. Elstrott, C.A. Boswell, Y. Zhang, W. Luk, Y. Lu, M.S. Dennis, R.M. Weimer, I. Chung, R.J. Watts, Transferrin receptor (TfR) trafficking determines brain uptake of TfR antibody affinity variants, *J. Exp. Med.* 211 (2014) 233–244, <https://doi.org/10.1084/jem.20131660>.
- [125] Y.J. Yu, J.K. Atwal, Y. Zhang, R.K. Tong, K.R. Wildsmith, C. Tan, N. Bien-Ly, M. Hersom, J.A. Maloney, W.J. Meilandt, D. Bumbaca, K. Gadkar, K. Hoyte, W. Luk, Y. Lu, J.A. Ernst, K. Searce-Lewie, J.A. Couch, M.S. Dennis, R.J. Watts, Therapeutic bispecific antibodies cross the blood-brain barrier in nonhuman primates, *Sci. Transl. Med.* 6 (2014), <https://doi.org/10.1126/SCITRANSLMED.3009835>.
- [126] W.M. Pardridge, Kinetics of blood-brain barrier transport of monoclonal antibodies targeting the insulin receptor and the transferrin receptor, *Pharmaceuticals (Basel)* 15 (2021), <https://doi.org/10.3390/PHI5010003>.
- [127] S.C. Christensen, D. Hudecz, A. Jensen, S. Christensen, M.S. Nielsen, Basigin antibodies with capacity for drug delivery across brain endothelial cells, *Mol. Neurobiol.* 58 (2021) 4392–4403, <https://doi.org/10.1007/S12035-021-02421-X>.
- [128] B. Zhang, X. Sun, H. Mei, Y. Wang, Z. Liao, J. Chen, Q. Zhang, Y. Hu, Z. Pang, X. Jiang, LDLR-mediated peptide-22-conjugated nanoparticles for dual-targeting therapy of brain glioma, *Biomaterials* 34 (2013) 9171–9182, <https://doi.org/10.1016/J.BIOMATERIALS.2013.08.039>.
- [129] W. Wong, Transporting leptin to its targets, *Sci. Signal.* 14 (2021), <https://doi.org/10.1126/SCISIGNAL.ABM4425>.
- [130] W. Zhang, Q.Y. Liu, A.S. Haqqani, S. Leclerc, Z. Liu, F. Fauteux, E. Baumann, C. E. Delaney, D. Ly, A.T. Star, E. Brunette, C. Sodja, M. Hewitt, J.K. Sandhu, D. B. Stanimirovic, Differential expression of receptors mediating receptor-mediated transcytosis (RMT) in brain microvessels, brain parenchyma and peripheral tissues of the mouse and the human, *Fluids Barriers CNS* 17 (2020) 47, <https://doi.org/10.1186/S12987-020-00209-0>.
- [131] M.E. Leunissen, R. Dreyfus, R. Sha, N.C. Seeman, P.M. Chaikin, Quantitative study of the association thermodynamics and kinetics of DNA-coated particles for different functionalization schemes, *J. Am. Chem. Soc.* 132 (2010) 1903–1913, <https://doi.org/10.1021/JA907919J>.
- [132] X. Tian, S. Angioletti-Uberti, G. Battaglia, On the design of precision nanomedicines, *Sci. Adv.* 6 (2020), <https://doi.org/10.1126/sciadv.aat0919>.
- [133] K.C. Tjandra, P. Thordarson, Multivalency in drug delivery—when is it too much of a good thing? *Bioconjug. Chem.* 30 (2019) 503–514, <https://doi.org/10.1021/acs.bioconjchem.8b00804>.

- [134] M.-H. Li, S.K. Choi, P.R. Leroueil, J.R. Baker, Evaluating binding avidities of populations of heterogeneous multivalent ligand-functionalized nanoparticles, *ACS Nano* 8 (2014) 5600–5609, <https://doi.org/10.1021/nn406455s>.
- [135] H. Bila, K. Paloja, V. Caroprese, A. Kononenko, M.M.C. Bastings, Multivalent pattern recognition through control of nano-spacing in low-valency super-selective materials, *J. Am. Chem. Soc.* 144 (2022) 21576–21586, <https://doi.org/10.1021/JACS.2C08529>.
- [136] O. Vilanova, J.J. Mittag, P.M. Kelly, S. Milani, K.A. Dawson, J.O. Rädler, G. Franzese, Understanding the kinetics of protein-nanoparticle corona formation, *ACS Nano* 10 (2016) 10842–10850, <https://doi.org/10.1021/ACS.NANO.6B04858>.
- [137] A. Cox, P. Andreozzi, R. Dal Magro, F. Fiordaliso, A. Corbelli, L. Talamini, C. Chinello, F. Raimondo, F. Magni, M. Tringali, S. Krol, P. Jacob Silva, F. Stellacci, M. Masserini, F. Re, Evolution of nanoparticle protein corona across the blood-brain barrier, *ACS Nano* 12 (2018) 7292–7300, <https://doi.org/10.1021/ACS.NANO.8B03500>.
- [138] S. Wang, E.E. Dormidontova, Selectivity of ligand-receptor interactions between nanoparticle and cell surfaces, *Phys. Rev. Lett.* 109 (2012), <https://doi.org/10.1103/PhysRevLett.109.238102>.
- [139] D. Leckband, S. Sheth, A. Halperin, Grafted poly(ethylene oxide) brushes as nonfouling surface coatings, *J. Biomater. Sci. Polym. Ed.* 10 (1999) 1125–1147, <https://doi.org/10.1163/156856299X00720>.
- [140] E.B. Zhulina, T.M. Birshtein, O. V. Borisov, Curved polymer and polyelectrolyte brushes beyond the Daoud-Cotton model, *The European Physical Journal E* 2006 20:3 20 (2006) 243–256, doi: 10.1140/EPJE/12006-10013-5.
- [141] R. Villaseñor, M. Schilling, J. Sundaresan, Y. Lutz, L. Collin, Sorting tubules regulate blood-brain barrier transcytosis, *Cell Rep.* 21 (2017) 3256–3270, <https://doi.org/10.1016/j.celrep.2017.11.055>.
- [142] X. Tian, D.M. Leite, E. Scarpa, S. Nyberg, G. Fullstone, J. Forth, D. Matias, A. Apriceno, A. Poma, A. Duro-Castano, M. Vuyyuru, L. Harker-Kirschneck, A. Sarić, Z. Zhang, P. Xiang, B. Fang, Y. Tian, L. Luo, L. Rizzello, G. Battaglia, On the shuttling across the blood-brain barrier via tubule formation: Mechanism and cargo avidity bias, *Sci. Adv.* 6 (2020), <https://doi.org/10.1126/SCIADV.ABC4397>.
- [143] P.L. Kastiritis, A.M.J.J. Bonvin, On the binding affinity of macromolecular interactions: daring to ask why proteins interact, *J. R. Soc. Interface* 10 (2013), <https://doi.org/10.1098/RSIF.2012.0835>.
- [144] S.Y. Joshi, S.A. Deshmukh, A review of advancements in coarse-grained molecular dynamics simulations, *Mol. Simul.* 47 (2021) 786–803, <https://doi.org/10.1080/08927022.2020.1828583>.
- [145] X. Du, Y. Li, Y.L. Xia, S.M. Ai, J. Liang, P. Sang, X.L. Ji, S.Q. Liu, Insights into protein–ligand interactions: mechanisms, models, and methods, *Int. J. Mol. Sci.* 2016, Vol. 17, Page 144 17 (2016) 144, doi: 10.3390/IJMS17020144.
- [146] A. Stank, D.B. Kokh, J.C. Fuller, R.C. Wade, Protein binding pocket dynamics, *Acc. Chem. Res.* 49 (2016) 809–815, <https://doi.org/10.1021/acs.accounts.5b00516>.
- [147] B. Zhang, H. Li, K. Yu, Z. Jin, Molecular docking-based computational platform for high-throughput virtual screening, *CCF Trans. High Perform. Comput.* 4 (2022) 63–74, <https://doi.org/10.1007/S42514-021-00086-5>.
- [148] S. AlRawashdeh, K.H. Barakat, Applications of molecular dynamics simulations in drug discovery, *Methods Mol. Biol.* 2714 (2024) 127–141, https://doi.org/10.1007/978-1-0716-3441-7_7.
- [149] M. Baek, F. DiMaio, I. Anishchenko, J. Dauparas, S. Ovchinnikov, G.R. Lee, J. Wang, Q. Cong, L.N. Kinch, R. Dustin Schaeffer, C. Millán, H. Park, C. Adams, C. R. Glassman, A. DeGiovanni, J.H. Pereira, A.V. Rodrigues, A.A. Van Dijk, A. C. Ebrecht, D.J. Opperman, T. Sagmeister, C. Buhlheller, T. Pavkov-Keller, M. K. Rathinaswamy, U. Dalwadi, C.K. Yip, J.E. Burke, K. Christopher Garcia, N. V. Grishin, P.D. Adams, R.J. Read, D. Baker, Accurate prediction of protein structures and interactions using a three-track neural network, *Science* 373 (2021) (1979) 871–876, <https://doi.org/10.1126/science.abj8754>.
- [150] J. Jumper, R. Evans, A. Pritzel, T. Green, M. Figurnov, O. Ronneberger, K. Tunyasuvunakool, R. Bates, A. Židek, A. Potapenko, A. Bridgland, C. Meyer, S.A. A. Kohl, A.J. Ballard, A. Cowie, B. Romera-Paredes, S. Nikolov, R. Jain, J. Adler, T. Back, S. Petersen, D. Reiman, E. Clancy, M. Zielinski, M. Steinegger, M. Pacholska, T. Berghammer, S. Bodenstein, D. Silver, O. Vinyals, A.W. Senior, K. Kavukcuoglu, P. Kohli, D. Hassabis, Highly accurate protein structure prediction with AlphaFold, *Nature* 2021 596:7873 596 (2021) 583–589, doi: 10.1038/s41586-021-03819-2.
- [151] W. Humphrey, A. Dalke, K. Schulten, VMD: Visual molecular dynamics, *J. Mol. Graph.* 14 (1996) 33–38, [https://doi.org/10.1016/0263-7855\(96\)00018-5](https://doi.org/10.1016/0263-7855(96)00018-5).
- [152] T.I. Croll, B.J. Smith, M.B. Margets, J. Whittaker, M.A. Weiss, C.W. Ward, M. C. Lawrence, Higher-Resolution Structure of the Human Insulin Receptor Ectodomain: Multi-Modal Inclusion of the Insert Domain, *Structure* 24 (2016) 469–476, <https://doi.org/10.1016/j.jstr.2015.12.014>.
- [153] N. Eswar, B. John, N. Mirkovic, A. Fiser, V.A. Ilyin, U. Pieper, A.C. Stuart, M. A. Marti-Renom, M.S. Madhusudhan, B. Yerkovich, A. Sali, Tools for comparative protein structure modeling and analysis, *Nucleic Acids Res.* 31 (2003) 3375, <https://doi.org/10.1093/NAR/GKG543>.
- [154] M.S. Park, Molecular dynamics simulations of the human glucose transporter GLUT1, *PLoS One* 10 (2015), <https://doi.org/10.1371/JOURNAL.PONE.0125361>.
- [155] S. Shityakov, E. Salvador, G. Pastorin, C. Förster, Blood-brain barrier transport studies, aggregation, and molecular dynamics simulation of multiwalled carbon nanotube functionalized with fluorescein isothiocyanate, *Int. J. Nanomedicine* 10 (2015) 1703–1713, <https://doi.org/10.2147/IJN.S68429>.
- [156] J. Abramson, J. Adler, J. Dunger, R. Evans, T. Green, A. Pritzel, O. Ronneberger, L. Willmore, A.J. Ballard, J. Bambrick, S.W. Bodenstein, D.A. Evans, C.C. Hung, M. O'Neill, D. Reiman, K. Tunyasuvunakool, Z. Wu, A. Žemgulytė, E. Arvaniti, C. Beattie, O. Bertolli, A. Bridgland, A. Cherepanov, M. Congreve, A.I. Cowen-Rivers, A. Cowie, M. Figurnov, F.B. Fuchs, H. Gladman, R. Jain, Y.A. Khan, C.M.R. Low, K. Perlin, A. Potapenko, P. Savy, S. Singh, A. Stecula, A. Thillaisundaram, C. Tong, S. Yakneen, E.D. Zhong, M. Zielinski, A. Židek, V. Bapst, P. Kohli, M. Jaderberg, D. Hassabis, J.M. Jumper, Accurate structure prediction of biomolecular interactions with AlphaFold 3, *Nature* 2024 630:8016 630 (2024) 493–500, doi: 10.1038/s41586-024-07487-w.
- [157] T.F. Shay, E.E. Sullivan, X. Ding, X. Chen, S.R. Kumar, D. Goertsen, D. Brown, A. Crosby, J. Vielmetter, M. Borsos, D.A. Wolfe, A.W. Lam, V. Gradinaru, Primate-conserved carbonic anhydrase IV and murine-restricted LY6C1 enable blood-brain barrier crossing by engineered viral vectors, *Sci. Adv.* 9 (2023), <https://doi.org/10.1126/sciadv.adg6618>.
- [158] N.J. Abbott, M.E. Pizzo, J.E. Preston, D. Janigro, R.G. Thorne, The role of brain barriers in fluid movement in the CNS: is there a “glymphatic” system? *Acta Neuropathol.* 135 (2018) 387–407, <https://doi.org/10.1007/S00401-018-1812-4>.
- [159] L.B. Flexner, Some problems of the origin, circulation and absorption of the cerebrospinal fluid, *Doi: 10.1086/394447* 8 (1933) 397–422, doi: 10.1086/394447.
- [160] E. Syková, C. Nicholson, Diffusion in brain extracellular space, *Physiol. Rev.* 88 (2008) 1277, <https://doi.org/10.1152/PHYSREV.00027.2007>.
- [161] A.J. Smith, X. Yao, J.A. Dix, B.J. Jin, A.S. Verkman, Test of the “glymphatic” hypothesis demonstrates diffusive and aquaporin-4-independent solute transport in rodent brain parenchyma, *Elife* 6 (2017), <https://doi.org/10.7554/ELIFE.27679>.
- [162] K.E. Holter, B. Kehlet, A. Devor, T.J. Sejnowski, A.M. Dale, S.W. Omholt, O. P. Ottersen, E.A. Nagelhus, K.A. Mardal, K.H. Pettersen, Interstitial solute transport in 3D reconstructed neuropil occurs by diffusion rather than bulk flow, *Proc. Natl. Acad. Sci. U. S. A.* 114 (2017) 9894–9899, <https://doi.org/10.1073/PNAS.1706942114>.
- [163] S.B. Hladky, M.A. Barrand, Mechanisms of fluid movement into, through and out of the brain: evaluation of the evidence, *Fluids Barriers CNS* 11 (2014), <https://doi.org/10.1186/2045-8118-11-26>.
- [164] M.M. Faghhi, M.K. Sharp, Is bulk flow plausible in perivascular, paravascular and paravenous channels? *Fluids Barriers CNS* 15 (2018) <https://doi.org/10.1186/S12987-018-0103-8>.
- [165] J.J. Iliff, M. Nedergaard, Is there a cerebral lymphatic system? *Stroke* 44 (2013) S93, <https://doi.org/10.1161/STROKEAHA.112.678698>.
- [166] J.J. Iliff, H. Lee, M. Yu, T. Feng, J. Logan, M. Nedergaard, H. Benveniste, Brain-wide pathway for waste clearance captured by contrast-enhanced MRI, *J. Clin. Invest.* 123 (2013) 1299–1309, <https://doi.org/10.1172/JCI67677>.
- [167] J.J. Iliff, M. Wang, Y. Liao, B.A. Plogg, W. Peng, G.A. Gundersen, H. Benveniste, G.E. Vates, R. Deane, S.A. Goldman, E.A. Nagelhus, M. Nedergaard, A paravascular pathway facilitates CSF flow through the brain parenchyma and the clearance of interstitial solutes, including amyloid β , *Sci. Transl. Med.* 4 (2012) <https://doi.org/10.1126/SCITRANSLMED.3003748>.
- [168] L. Xie, H. Kang, Q. Xu, M.J. Chen, Y. Liao, M. Thiyagarajan, J. O'Donnell, D. J. Christensen, C. Nicholson, J.J. Iliff, T. Takano, R. Deane, M. Nedergaard, Sleep drives metabolite clearance from the adult brain, *Science* 342 (2013) 373–377, <https://doi.org/10.1126/SCIENCE.1241224>.
- [169] M. Demeule, J.C. Currie, Y. Bertrand, C. Ché, T. Nguyen, A. Régina, R. Gabathuler, J.P. Castaigne, R. Béliève, Involvement of the low-density lipoprotein receptor-related protein in the transcytosis of the brain delivery vector Angiopep-2, *J. Neurochem.* 106 (2008) 1534–1544, <https://doi.org/10.1111/J.1471-4159.2008.05492.X>.
- [170] R. Dal Magro, B. Albertini, S. Beretta, R. Rigolio, E. Donzelli, A. Chiorazzi, M. Ricci, P. Blasi, G. Sancini, Artificial apolipoprotein coronas enables nanoparticle brain targeting, *Nanomedicine* 14 (2018) 429–438, <https://doi.org/10.1016/j.nano.2017.11.008>.
- [171] A. Régina, M. Demeule, C. Ché, I. Lavallée, J. Poirier, R. Gabathuler, R. Béliève, J.P. Castaigne, Antitumour activity of ANG1005, a conjugate between paclitaxel and the new brain delivery vector Angiopep-2, *Br. J. Pharmacol.* 155 (2008) 185–197, <https://doi.org/10.1038/BJP.2008.260>.
- [172] P. Kumthekar, S.C. Tang, A.J. Brenner, S. Kesari, D.E. Piccioni, C. Anders, J. Carrillo, P. Chalasani, P. Kabos, S. Puhalla, K. Tkaczuk, A.A. Garcia, M. S. Ahluwalia, J.S. Wefel, N. Lakhani, M. Ibrahim, ANG1005, a brain-penetrating peptide–drug conjugate, shows activity in patients with breast cancer with leptomeningeal carcinomatosis and recurrent brain metastases, *Clin. Cancer Res.* 26 (2020) 2789–2799, <https://doi.org/10.1158/1078-0432.CCR-19-3258>.
- [173] F.C. Thomas, K. Taskar, V. Rudraraju, S. Goda, H.R. Thorsheim, J.A. Gaasch, R. K. Mittapalli, D. Palmieri, P.S. Steeg, P.R. Lockman, Q.R. Smith, Uptake of ANG1005, a novel paclitaxel derivative, through the blood-brain barrier into brain and experimental brain metastases of breast cancer, *Pharm. Res.* 26 (2009) 2486–2494, <https://doi.org/10.1007/S11095-009-9964-5>.
- [174] Y. Anami, W. Xiong, A. Yamaguchi, C.M. Yamazaki, N. Zhang, Z. An, K. Tsuchikama, Homogeneous antibody–angiopep 2 conjugates for effective brain targeting, *RSC Adv.* 12 (2022) 3359–3364, <https://doi.org/10.1039/D1RA08131D>.
- [175] X. Cai, A. Refaat, P.Y. Gan, B. Fan, H. Yu, S.H. Thang, C.J. Drummond, N. H. Voelcker, N. Tran, J. Zhai, Angiopep-2-functionalized lipid cubosomes for blood-brain barrier crossing and glioblastoma treatment, *ACS Appl. Mater. Interfaces* 16 (2024) 12161–12174, <https://doi.org/10.1021/ACSAMI.3C14709>.

- [176] H. Xu, C. Li, Y. Wei, H. Zheng, H. Zheng, B. Wang, J.G. Piao, F. Li, Angiopep-2-modified calcium arsenite-loaded liposomes for targeted and pH-responsive delivery for anti-glioma therapy, *Biochem. Biophys. Res. Commun.* 551 (2021) 14–20, <https://doi.org/10.1016/j.bbrc.2021.02.138>.
- [177] A. Zensi, D. Begley, C. Pontikis, C. Legros, L. Mihoreanu, S. Wagner, C. Büchel, H. von Briesen, J. Kreuter, Albumin nanoparticles targeted with Apo E enter the CNS by transcytosis and are delivered to neurones, *J. Control. Release* 137 (2009) 78–86, <https://doi.org/10.1016/J.JCONREL.2009.03.002>.
- [178] S. Arora, D. Sharma, J. Singh, GLUT-1: an effective target to deliver brain-derived neurotrophic factor gene across the blood brain barrier, *ACS Chem. Neurosci.* 11 (2020) 1620–1633, <https://doi.org/10.1021/ACSCHEMNEURO.0C00076>.
- [179] J.A. Couch, Y.J. Yu, Y. Zhang, J.M. Tarrant, R.N. Fuji, W.J. Meilandt, H. Solano, R.K. Tong, K. Hoyte, W. Luk, Y. Lu, K. Gadkar, S. Prabhu, B.A. Ordonia, Q. Nguyen, Y. Lin, Z. Lin, M. Balazs, K. Searce-Levie, J.A. Ernst, M.S. Dennis, R. J. Watts, Addressing safety liabilities of TfR bispecific antibodies that cross the blood-brain barrier, *Sci. Transl. Med.* 5 (2013), <https://doi.org/10.1126/SCITRANSLMED.3005338>.
- [180] Y.J. Yu, Y. Zhang, M. Kenrick, K. Hoyte, W. Luk, Y. Lu, J. Atwal, J.M. Elliott, S. Prabhu, R.J. Watts, M.S. Dennis, Boosting brain uptake of a therapeutic antibody by reducing its affinity for a transcytosis target, *Sci. Transl. Med.* 3 (2011), <https://doi.org/10.1126/SCITRANSLMED.3002230>.
- [181] C. Díaz-Perlas, B. Oller-Salvia, M. Sánchez-Navarro, M. Teixidó, E. Giralt, Branched BBB-shuttle peptides: chemoselective modification of proteins to enhance blood–brain barrier transport, *Chem. Sci.* 9 (2018) 8409–8415, <https://doi.org/10.1039/C8SC02415D>.
- [182] H. Sonoda, H. Morimoto, E. Yoden, Y. Koshimura, M. Kinoshita, G. Golovina, H. Takagi, R. Yamamoto, K. Minami, A. Mizoguchi, K. Tachibana, T. Hirato, K. Takahashi, A blood-brain-barrier-penetrating anti-human transferrin receptor antibody fusion protein for neuronopathic mucopolysaccharidosis II, *Mol. Ther.* 26 (2018) 1366, <https://doi.org/10.1016/J.YMTHE.2018.02.032>.
- [183] T. Okuyama, Y. Eto, N. Sakai, K. Minami, T. Yamamoto, H. Sonoda, M. Yamaoka, K. Tachibana, T. Hirato, Y. Sato, Iduronate-2-sulfatase with anti-human transferrin receptor antibody for neuropathic mucopolysaccharidosis II: a phase 1/2 trial, *Mol. Ther.* 27 (2018) 456, <https://doi.org/10.1016/J.YMTHE.2018.12.005>.
- [184] M.S. Kariolis, R.C. Wells, J.A. Getz, W. Kwan, C.S. Mahon, R. Tong, D.J. Kim, A. Srivastava, C. Bedard, K.R. Henne, T. Giese, V.A. Assimon, X. Chen, Y. Zhang, H. Solano, K. Jenkins, P.E. Sanchez, L. Kane, T. Miyamoto, K.S. Chew, M. E. Pizzo, N. Liang, M.E.K. Calvert, S.L. DeVos, S. Baskaran, S. Hall, Z.K. Sweeney, R.G. Thorne, R.J. Watts, M.S. Dennis, A.P. Silverman, Y.J.Y. Zuchero, Brain delivery of therapeutic proteins using an Fc fragment blood-brain barrier transport vehicle in mice and monkeys, *Sci. Transl. Med.* 12 (2020), <https://doi.org/10.1126/SCITRANSLMED.AAY1359>.
- [185] J.C. Ullman, A. Arguello, J.A. Getz, A. Bhalla, C.S. Mahon, J. Wang, T. Giese, C. Bedard, D.J. Kim, J.R. Blumenfeld, N. Liang, R. Ravi, A.A. Nugent, S.S. Davis, C. Ha, J. Duque, H.L. Tran, R.C. Wells, S. Lianoglou, V.M. Daryani, W. Kwan, H. Solano, H. Nguyen, T. Earr, J.C. Dugas, M.D. Tuck, J.L. Harvey, M.L. Reyzer, R.M. Caprioli, S. Hall, S. Poda, P.E. Sanchez, M.S. Dennis, K. Gunasekaran, A. Srivastava, T. Sandmann, K.R. Henne, R.G. Thorne, G. Di Paolo, G. Astarita, D. Diaz, A.P. Silverman, R.J. Watts, Z.K. Sweeney, M.S. Kariolis, A.G. Henry, Brain delivery and activity of a lysosomal enzyme using a blood-brain barrier transport vehicle in mice, *Sci. Transl. Med.* 12 (2020), <https://doi.org/10.1126/SCITRANSLMED.AAY1163>.
- [186] A. Arguello, C.S. Mahon, M.E.K. Calvert, D. Chan, J.C. Dugas, M.E. Pizzo, E. R. Thomsen, R. Chau, L.A. Damo, J. Duque, M. Fang, T. Giese, D.J. Kim, N. Liang, H.N. Nguyen, H. Solano, B. Tsogtbaatar, J.C. Ullman, J. Wang, M.S. Dennis, D. Diaz, K. Gunasekaran, K.R. Henne, J.W. Lewcock, P.E. Sanchez, M.D. Troyer, J. M. Harris, K. Searce-Levie, L. Shan, R.J. Watts, R.G. Thorne, A.G. Henry, M. S. Kariolis, Molecular architecture determines brain delivery of a transferrin receptor-targeted lysosomal enzyme, *J. Exp. Med.* 219 (2022), <https://doi.org/10.1084/JEM.20211057>.
- [187] A. Arguello, R. Meisner, E.R. Thomsen, H.N. Nguyen, R. Ravi, J. Simms, I. Lo, J. Speckart, J. Holtzman, T.M. Gill, D. Chan, Y. Cheng, C.L. Chiu, J.C. Dugas, M. Fang, I.A. Lopez, H. Solano, B. Tsogtbaatar, Y. Zhu, A. Bhalla, K.R. Henne, A. G. Henry, A. Delucchi, S. Costanzo, J.M. Harris, D. Diaz, K. Searce-Levie, P. E. Sanchez, Iduronate-2-sulfatase transport vehicle rescues behavioral and skeletal phenotypes in a mouse model of Hunter syndrome, *JCI Insight* 6 (2021), <https://doi.org/10.1172/JCI.INSIGHT.145445>.
- [188] A.S. Haqqani, G. Thom, M. Burrell, C.E. Delaney, E. Brunette, E. Baumann, C. Sodja, A. Jezierski, C. Webster, D.B. Stanimirovic, Intracellular sorting and transcytosis of the rat transferrin receptor antibody OX26 across the blood–brain barrier in vitro is dependent on its binding affinity, *J. Neurochem.* 146 (2018) 735, <https://doi.org/10.1111/JNC.14482>.
- [189] R.J. Boado, J.Z. Lu, E.K.W. Hui, W.M. Pardridge, Reduction in brain heparan sulfate with systemic administration of an IgG trojan horse-sulfamidase fusion protein in the mucopolysaccharidosis type IIIA mouse, *Mol. Pharm.* 15 (2018) 602–608, <https://doi.org/10.1021/ACS.MOLPHARMACEUT.7B00958>.
- [190] W. Alata, A. Yogi, E. Brunette, C.E. Delaney, H. van Faassen, G. Hussack, U. Iqbal, K. Kemmerich, A.S. Haqqani, M.J. Moreno, D.B. Stanimirovic, Targeting insulin-like growth factor-1 receptor (IGF1R) for brain delivery of biologics, *FASEB J.* 36 (2022) e22208, <https://doi.org/10.1096/FJ.202101644R>.
- [191] Y.J.Y. Zuchero, X. Chen, N. Bien-Ly, D. Bumbaca, R.K. Tong, X. Gao, S. Zhang, K. Hoyte, W. Luk, M.A. Huntley, L. Phu, C. Tan, D. Kallop, R.M. Weimer, Y. Lu, D. S. Kirkpatrick, J.A. Ernst, B. Chih, M.S. Dennis, R.J. Watts, Discovery of novel blood-brain barrier targets to enhance brain uptake of therapeutic antibodies, *Neuron* 89 (2016) 70–82, <https://doi.org/10.1016/J.NEURON.2015.11.024>.
- [192] S.C. Christensen, B.O. Krogh, A. Jensen, C.B.F. Andersen, S. Christensen, M.S. Nielsen, Characterization of basigin monoclonal antibodies for receptor-mediated drug delivery to the brain, *Scientific Reports* 2020 10:1 10 (2020) 1–13. doi: 10.1038/s41598-020-71286-2.
- [193] W.M. Pardridge, R.J. Boado, R. Giugliani, M. Schmidt, Plasma pharmacokinetics of valanafusp alpha, a human insulin receptor antibody-iduronidase fusion protein, patients with mucopolysaccharidosis type I, *BioDrugs* 32 (2018) 169–176, <https://doi.org/10.1007/S40259-018-0264-7>.
- [194] R. Giugliani, L. Giugliani, F. De Oliveira Poswar, K.C. Donis, A.D. Corte, M. Schmidt, R.J. Boado, I. Nestrail, C. Nguyen, S. Chen, W.M. Pardridge, Neurocognitive and somatic stabilization in pediatric patients with severe Mucopolysaccharidosis Type i after 52 weeks of intravenous brain-penetrating insulin receptor antibody-iduronidase fusion protein (valanafusp alpha): an open label phase 1-2 trial, *Orphanet J. Rare Dis.* 13 (2018) 1–11, <https://doi.org/10.1186/S13023-018-0849-8>.
- [195] J.Z. Lu, R.J. Boado, E.K.W. Hui, Q.H. Zhou, W.M. Pardridge, Expression in CHO cells and pharmacokinetics and brain uptake in the rhesus monkey of an IgG-iduronate-2-sulfatase fusion protein, *Biotechnol. Bioeng.* 108 (2011) 1954, <https://doi.org/10.1002/BIT.23118>.
- [196] R.J. Boado, E. Ka-Wai Hui, J. Zhiqiang Lu, W.M. Pardridge, Insulin receptor antibody-iduronate 2-sulfatase fusion protein: pharmacokinetics, anti-drug antibody, and safety pharmacology in Rhesus monkeys, *Biotechnol Bioeng* 111 (2014) 2317–2325, <https://doi.org/10.1002/BIT.25289>.
- [197] Y.C. Kuo, C.Y. Chung, Transcytosis of CRM197-grafted polybutylcyanoacrylate nanoparticles for delivering zidovudine across human brain-microvascular endothelial cells, *Colloids Surf. B Biointerfaces* 91 (2012) 242–249, <https://doi.org/10.1016/J.COLSURFB.2011.11.007>.